Environmental and climatic changes in the Jura mountains (eastern France) during the Lateglacial–Holocene transition: a multi-proxy record from Lake Lautrey

Michel Magny[a], Gerard Aalbersberg[b], Carole Bégeot[a], Pascale Benoit-Ruffaldi[a], Gilles Bossuet[a], Jean-Robert Disnar[c], Oliver Heiri[d], Fatima Laggoun-Defarge[c], Florence Mazier[a], Laurent Millet[a], Odile Peyron[a], Boris Vannière[a] and Anne-Véronique Walter-Simonnet[a]

[a]*UMR 6565-CNRS, Faculty of Sciences, 16 route de Gray, 25 030 Besançon, France*
[b]*Faculty of Earth and Life Sciences, Vrije Universiteit Amsterdam, De Boelelaan 1085, 1081 HV Amsterdam, The Netherlands*
[c]*ISTO UMR 6113-CNRS, University of' Orleans, Bâtiment Geosciences, BP 6759, Rue de St Amand, 45067 ORLEANS Cedex 2, France*
[d]*Utrecht University, Palaeoecology, Laboratory of Palaeobotany and Palynology, Budapestlaan 4, 3584 CD Utrecht, The Netherlands*

Abstract

This paper presents a multi-proxy reconstruction of the climatic and environmental changes during the Last Glacial–Interglacial transition as recorded by a sediment sequence from Lake Lautrey (Jura, eastern France). This reconstruction is based on analysis of pollen, chironomid, organic matter, oxygen-isotope, mineralogical, magnetic susceptibility and inferred lake-level data at a high temporal resolution. The chronology is derived using AMS radiocarbon dates, the position of the Laacher See Tephra (LST), and of correlation between the Lautrey and GRIP oxygen-isotope records. This data set reveals a detailed sequence of environmental changes in the Jura mountains from Greenland Stadial 2a to the early Holocene. Biotic and abiotic indicators allow the recognition of major abrupt changes associated with the GS-2a/GI-1e, GI-1a/GS-1 and GS-1/Preboreal transitions, and other minor fluctuations related to the cold events GI-1d, GI-1b and the Preboreal oscillation (PBO). They also suggest additional cooling spells at ca 14,550 and 14,350 cal yr BP (Intra-Bølling Cold Periods), at ca 13,500 and ca 12,700 cal yr BP just before the GS-1 onset, and at ca 11,350 cal yr BP just before the PBO, as well as an intriguing brief warming episode within GS-1 at ca 12,080 cal yr BP. Summer temperature increased by ca 5 °C at the start of GI-1e, and by 1.5–3 °C at the Holocene onset, while it decreased by ca 3–4 °C at the beginning of GS-1. Major changes in local hydrology and in seasonality appear to be also associated with the GS-2a/GI-1e, GI-1a/GS-1 and GS-1/Preboreal transitions. Pollen and abiotic indicators suggest a greater sensitivity of the vegetation cover to climatic oscillations during the first part of the Lateglacial Interstadial than during the second part (after ca 13,700 cal yr BP), when a closed forest had been restored in this area. By contrast, the restoration of forest cover took less than 300 yr after the end of GS-1. At the beginning of GI-1e and GS-1, no lag occurs (within the sampling resolution of 20–50 yr) in the responses of aquatic (chironomids) and terrestrial (pollen) ecosystems, while, at the onset of the Holocene, the response of the vegetation appears slightly delayed in comparison with that of the chironomid community. Finally, the recognition of two successive tephra layers, which were deposited just before the LST at ca 12,950 cal yr BP and which originated from Le Puy de la Nugère (Massif Central, France),

provides an additional tephrochronological tool for correlation between Lateglacial European sequences.

1. Introduction

Since the Last Glacial–Interglacial transition was marked by rapid and pronounced climatic oscillations associated with successive climatic steps during general deglaciation (Lowe, 1994; Björck et al., 1996; Clark et al., 2001), many investigations have focused on this period. Stimulated by the high-resolution records obtained from the Greenland ice-cores (Johnsen et al., 1992), increasing efforts are now being undertaken to quantify Lateglacial climatic changes and to improve the temporal resolution and chronology of multi-proxy continental records. In particular, it is crucial to obtain better correlations between terrestrial, marine and ice-sheet records and to improve our understanding of the responses of terrestrial environments to rapid climatic changes (Björck et al., 1998; Brauer et al., 1999; Ammann et al., 2000; Birks and Wright, 2000; Walker et al., 2003).

As a contribution to such efforts, this paper presents the results of a multidisciplinary study undertaken at Lake Lautrey in the Jura mountains. The investigation is part of a project funded by the program ECLIPSE (Past Environments and Climates) of the French CNRS to establish and compare high-resolution records between west-central Europe and the north-western Mediterranean region. Using an integrated approach, based on a range of biotic and abiotic indicators (pollen, chironomids, organic matter (OM), oxygen-isotopes, mineralogy, magnetic susceptibility (MS), lake-level fluctuations), the aim is to establish a multi-proxy record of environmental and climatic changes from GS-2a to the early Holocene. Major climatic changes during this period have been quantified using chironomid, pollen and lake-level data.

2. The site

2.1. Location

Lake Lautrey (46°35′14″N; 5°51′50″E) is located at 788 m above sea level (a.s.l.) in the Jura mountains (eastern France) (Fig. 1). It is a small residual lake (75×40 m^2, 1900 m^2) surrounded by mires as a result of overgrowing processes. Its catchment area covers ca 2 km^2, and is underlain by Jurassic and Cretaceous limestones with outcrops of dolomite. It is characterised by hills culminating at ca 830 m covered by *Abies* and *Fagus* forest. The mean temperature is −1 °C in the coldest month and 16 °C in the warmest month, with annual precipitation reaching ca 1500 mm. The lake is fed by small streams and runoff from the catchment area. After a short surface course, its outlet descends into a karstic cavity to flow underground.

Systematic lithostratigraphic investigations based on a grid of 37 cores with sampling points every 50 m (Fig. 2) have shown that, during the Lateglacial period, the lake size was ca 500×200 m^2 with a maximum water depth of 12 m (Bossuet et al., 1997 and Bossuet et al., 2000).

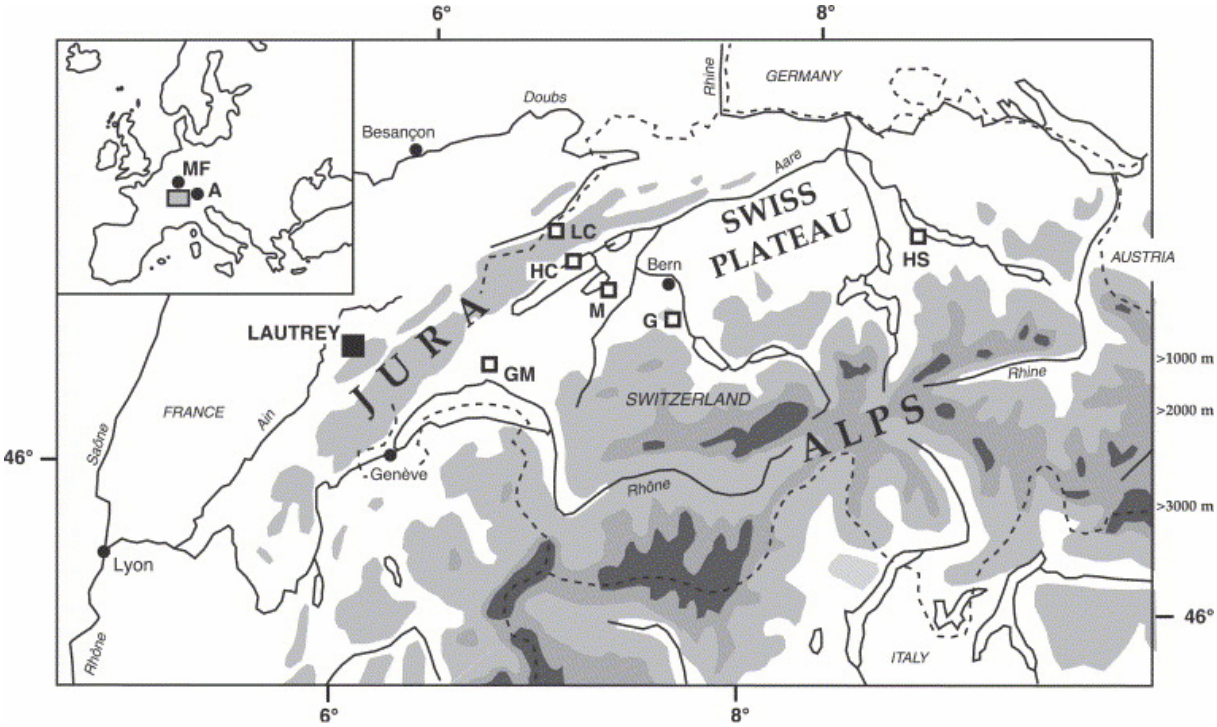

Fig. 1. Location of Lake Lautrey in west-central Europe. G, Gerzensee; GM, Grand-Marais; HC, Hauterive-Champréveyres (Lake Neuchâtel); HS, Horgen-Scheller (Zürichsee); LC, Lake Le Locle; M, Montilier (Lake Morat). Insert: A, Ammersee; MF, Merfelder Maar.

This first exploration coupled with pollen stratigraphy has also revealed an infilling sediment sequence (Fig. 2) which is typical for this region, with (1) late Pleniglacial clayey silts at the base, (2) biogenic carbonate lake-marl in the middle sector (Lateglacial Interstadial and Holocene), the deposition of which was interrupted by the accumulation of clayey silts during the Younger Dryas event (GS-1), and (3) organic sediments (gyttja and peat) at the top (final overgrowing step). Furthermore, the Laacher See Tephra (LST) was observed in the upper part of the Lateglacial Interstadial (GI-1) deposits (Bossuet et al., 1997; Vanniere et al., 2004).

2.2. Stratigraphy

Point 6 in the north-eastern part of the lacustrine basin (Fig. 2) was chosen for the multidisciplinary study presented here, as a best compromise meeting the various requirements of the different proxy investigations involved in the project. Two overlapping twin cores were taken with a Russian peat corer of 10 cm diameter and 100 cm length. The stratigraphy was as follows (Fig. 2):

• *Sediment unit 1 (500–445 cm)*: Clayey silts, dark-grey in colour.

• *Sediment unit 2 (445–326 cm)*: Clayey biogenic carbonate lake-marl, yellow-green in colour from 445 to 430 cm, and silty biogenic carbonate lake-marl, yellow-beige in colour from 430 to 326 cm with the LST at 345 cm.

• *Sediment unit 3 (326–298 cm)*: Clayey silts grey in colour from 325 to 311 cm, and alternating layers of grey clayey silts and yellow-beige biogenic lake-marl from 311 to 298 cm.

• *Sediment unit 4 (298–229 cm)*: Yellow-beige authigenic lake marl.

• *Sediment unit 5 (229–0 cm)*: Gyttja and peat.

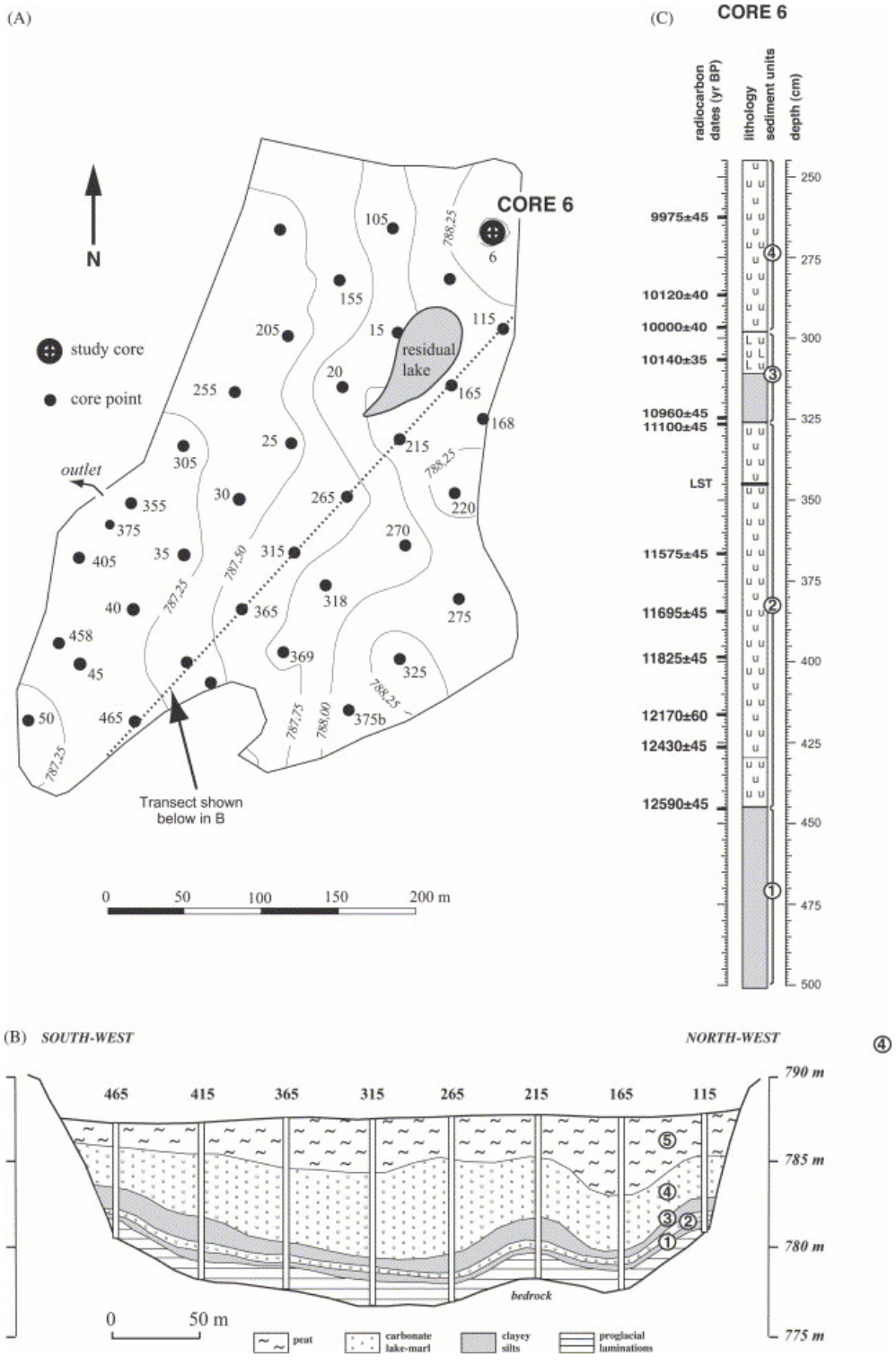

Fig. 2. (A) Map of the Lautrey mire showing the surface altimetry (m a.s.l.) and the location of the coring points for the site exploration. (B) Axial cross section from point 115 to point 465, i.e. through the deepest parts of the lacustrine basin (Bossuet et al., 2000). (C) Sediment profile of Lautrey core 6 used for this study, with an indication of the position of LST and samples for radiocarbon dating.

Lithostratigraphic correlations, previous pollen studies and the position of the LST (Bossuet et al., 1997) indicate that sediments units 1, 2, 3 and 4 correspond to the Oldest Dryas, Bølling–Allerød, Younger Dryas and Preboreal biozones (Ammann and Lotter, 1989), respectively.

2.3. Sampling and analytical strategy

After measurement of the volume MS at 0.5 cm intervals, contiguous samples were taken at 1 cm intervals in the Oldest Dryas, Bølling–Allerød and Preboreal sections. Samples were removed at 0.5 cm intervals from the Younger Dryas section due to a generally weaker sedimentation rate during the Younger Dryas event as observed in previous regional studies (Bégeot, 2000). To allow an integrated approach, every sample was cut into seven portions for pollen, chironomid, lake-level, mineralogy, grain-size, isotope and OM analyses.

3. Chronology

The chronology of the Lautrey core 6 sediment sequence is based on the following evidence:

• Twelve AMS radiocarbon dates from terrestrial plant macrofossils (Table 1 and Fig. 2C). The ^{14}C ages have been calibrated using IntCal 4.3 (Stuiver et al., 1998). The radiocarbon ages obtained appear consistent with the regional Lateglacial pollen zones defined by de Beaulieu et al. (1994) and Bégeot (2000) for the Jura mountains.

• The 1 mm thick ash layer of LST was identified at 345 cm depth in core 6. On the basis of petrographic and SEM observations, the mineral composition of this tephra layer has been extensively published elsewhere (Bossuet et al., 1997; Vanniere et al., 2004). It has been radiocarbon dated to 11,063±12 ^{14}C yr BP (Friedrich et al., 1999). Ammann et al. (2000) suggested an age of 12,836 cal yr BP based on correlation between the Gerzensee and GRIP oxygen-isotope records, and Brauer et al. (1999) estimated an age of 12,880 cal yr BP from varve counts in the Meerfelder Maar (Germany).

4. Pollen analysis

4.1. Laboratory methods

Samples were analysed at 1 or 2 cm intervals and treated by standard methods, including HCl, HF, NaOH and acetolysis. The pollen preservation was good and concentrations (calculated using a volumetric method; Cour, 1974) were always sufficient to count over 500 pollen grains per slide. Pollen percentages are based on the pollen sum of arboreal (AP) and non-arboreal (NAP) pollen grains, excluding spores.

Table 1. : AMS radiocarbon dates obtained from core 6 of Lake Lautrey

Depth (cm)	**Radiocarbon age (yr BP)**	**Calibrated age (2σ) (cal yr BP)**	**Laboratory number (Vienne)**	**Material**
262	9975±45	11,904–11,130	VERA-1717	Wood fragments
286	10,120±40	12,269–11,358	VERA-1722	Wood fragments
296	10,000±40	11,918–11,257	VERA-1716	Wood fragments
305	10,140±35	12,282–11,442	VERA-1715	Wood fragments
324	10,960±45	13,154–12,657	VERA-1724	Wood fragments
326	11,100±45	14,191–12,683	VERA-1725	Wood fragments
366	11,575±45	13,836–13,317	VERA-1726	Wood fragments
384	11,695±45	15,092–13,442	VERA-1727	Wood fragments
398	11,825±45	15,205–13,587	VERA-1728	Wood fragments
416	12,170±60	15,400–13,836	POZ-4496	Wood fragments
426	12,430±45	15,517–14,139	VERA-1729	Wood fragments
445	12,590±45	15,592–14,223	VERA-1730	Wood fragments

4.2. The pollen record

Fig. 3 and Fig. 4 show percentage and concentration data for selected principal taxa. The major changes in these diagrams led to the definition of six local pollen assemblage zones (LPAZ) as follows.

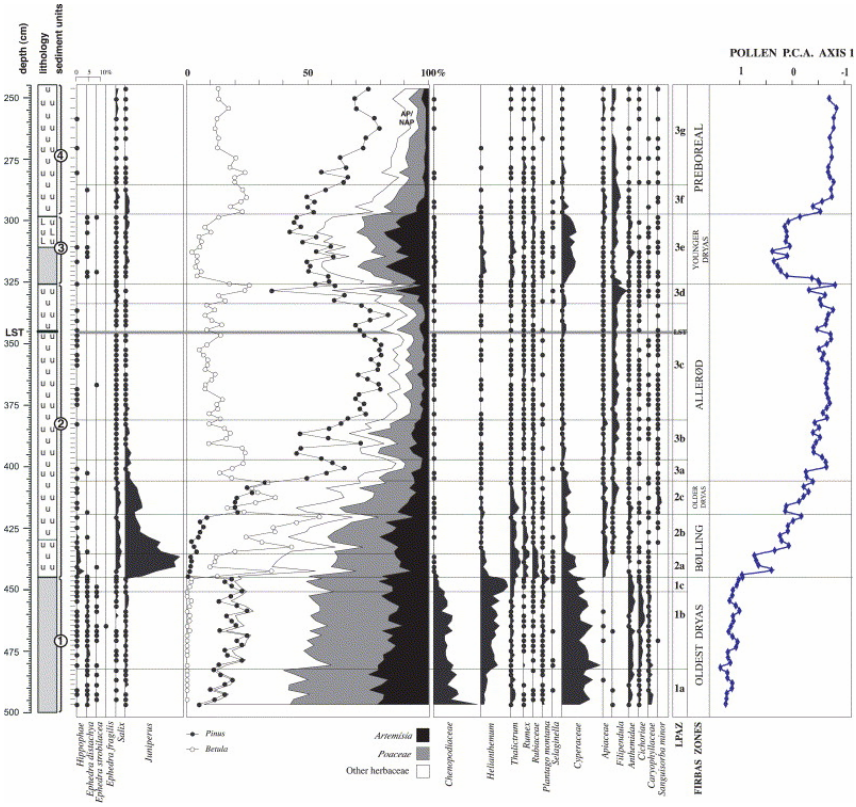

Fig. 3. Percentage pollen diagram from Lautrey core 6 (main taxa only shown). Analysis: P. Ruffaldi. Pollen PCA axis 1: see explanations in Section 12.2.

Taken as a whole, LPAZ-1 (500–445 cm) is dominated by high percentages of herbaceous taxa, mainly *Artemisia*, Poaceae and other heliophilous taxa, such as Chenopodiaceae and *Helianthemum* as well as Cyperaceae. Generally speaking, pollen concentrations remain low. The relatively high percentages of *Pinus* (ca 25%) are interpreted as due to long-distance transport. These data indicate an open herbaceous landscape and can be correlated with the Oldest Dryas pollen zone (de Beaulieu et al., 1994).

Within LAPZ-1, subzone LPAZ-1b (480–454.5 cm) can be distinguished from LPAZ-1a (500–480 cm) on the basis of an increase in the percentage values of *Helianthemum* and in concentrations of herbaceous taxa. *Pinus* also shows a slight increase in the percentages but its concentrations values remain low. This general picture suggests a possible local expansion of the grassland vegetation, particularly at the upper part of subzone LPAZ-1b where the concentration values of herb taxa rapidly increase. These features are reinforced in subzone LPAZ-1c (450–445 cm) with *Helianthemum* values peaking at 12%.

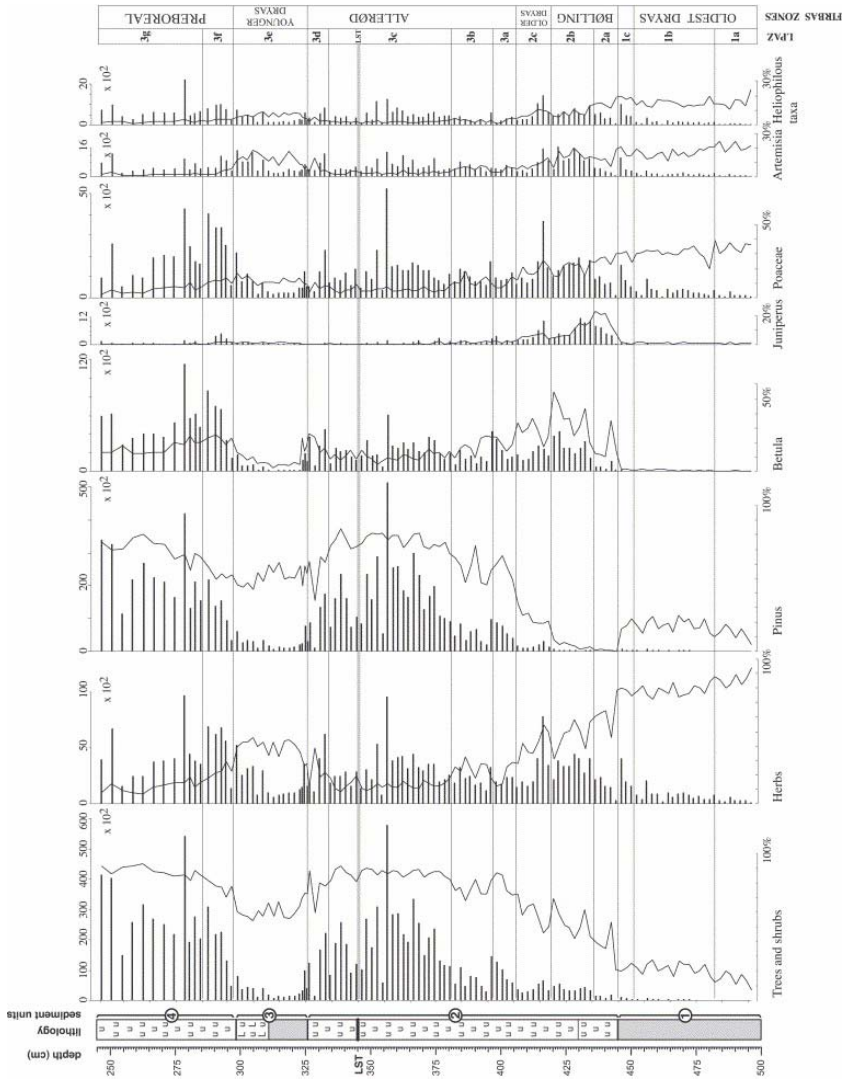

Fig. 4. Concentration pollen diagram from Lautrey core 6 (histograms). The curves present the percentage values from Fig. 3. Analysis: P. Ruffaldi.

LPAZ-2a (*Betula–Juniperus* zone, 444.5–436.5 cm) is marked at its beginning by a strong increase in percentages and concentrations of juniper typical of the onset of the Bølling pollen zone (de Beaulieu et al., 1994). The development of a shrub vegetation is also indicated by the presence of *Salix* and *Hippophaë* which reach maxima. Just after the first rapid expansion of *Juniperus*, *Betula* shows a conspicuous short maximum in percentage and concentration data before decreasing abruptly.

LPAZ-2b (*Betula* zone, 436.5–420.5 cm) is characterised by the establishment of a birch woodland as indicated by high percentages and concentrations of *Betula*, while *Juniperus* retreats (second part of the Bølling pollen zone). The diagrams also show a moderate fall in percentages of *Betula* (at around level 428 cm) concomitant with higher values of *Artemisia* and herbs. This may reflect a short regressive phase in vegetation development during this period, which previously has been recognised in most of pollen diagrams obtained from sites in the Jura mountains (Bégeot, 2000). During LPAZ-2c (420.5–406.5 cm), a marked regressive phase is registered by two successive decreases in *Betula* percentages and concentrations. The first was associated with an increase in grasses at the beginning of the

subzone and a re-expansion of juniper, and the second with a decrease in AP concentrations. The relative decline of birch woodland appears to have favoured a simultaneous development of *Pinus*. This regressive phase at the transition between the Bølling and Allerød pollen zones is assigned to the Older Dryas pollen zone (Lotter et al., 1992; de Beaulieu et al., 1994).

LPAZ-3 (420.5–245 cm) is identified by the dominance of *Pinus*. It is correlated with the Allerød, Younger Dryas and Preboreal pollen zones and is divided into seven subzones. LPAZ-3a shows a rapid rise and domination of *Pinus* percentages indicating the regional extension of pine forests. LPAZ-3b marks two successive interruptions of this expansion with declines of *Pinus* percentages and concentrations concomitant with a 5% increase in *Artemisia* percentages while juniper reaches 3% (regressive phases). LPAZ-3c displays a considerable dominance of *Pinus* in the percentage diagram. After a continuing expansion of the pine forests until 356.5 cm depth, a strong reduction in pollen concentrations can be observed, in particular at levels 354.5 and 346.5–342.5 cm. During LPAZ-3d, the *Pinus* dominance is affected by a regression well marked in sample 328.5 cm by a strong reduction of *Pinus* percentages and concentrations, while *Betula* and *Artemisia* percentages increase.

After a partial recovery in terms of percentages and concentrations, all the evidence points to a marked long-lasting regression of the vegetation during LPAZ-3e (325.75–296.5 cm). A rise in NAP percentages, mainly *Artemisia*, Chenopodiaceae, *Helianthemum*, Poaceae and Cyperaceae, associated with a strong decrease in AP concentrations, indicates a reduction of the pine-birch forests and an expansion of open habitats and can be correlated with the Younger Dryas pollen zone (de Beaulieu et al., 1994). Before the abrupt decrease in NAP percentages at the end of LPAZ-3e, the AP and NAP pollen concentrations show a progressive increase during the upper part of this biozone.

LPAZ-3f (296.5–250 cm) is marked by a rapid re-expansion of the pine-birch woodland at the Younger Dryas/Preboreal transition. The percentage diagram indicates an increase in *Betula*, *Pinus*, *Juniperus* and *Salix* while Poaceae*, Artemisia*, Cyperaceae and most other heliophilous taxa decrease. The AP (and to a lesser extent, NAP) concentrations increase rapidly. During LPAZ-3g, the pine forests became more dense whereas *Betula*, *Juniperus* and *Salix* as well as NAP concentrations decline.

5. Chironomid analysis

The chironomid stratigraphy established from Lautrey core 6 for the Last Glacial–Interglacial transition has already been presented and discussed in previous papers (Millet et al., 2003; Heiri and Millet, 2005). For this study, the original chironomid record has been extended by 13 additional samples to extend the record for the Preboreal (Fig. 5).

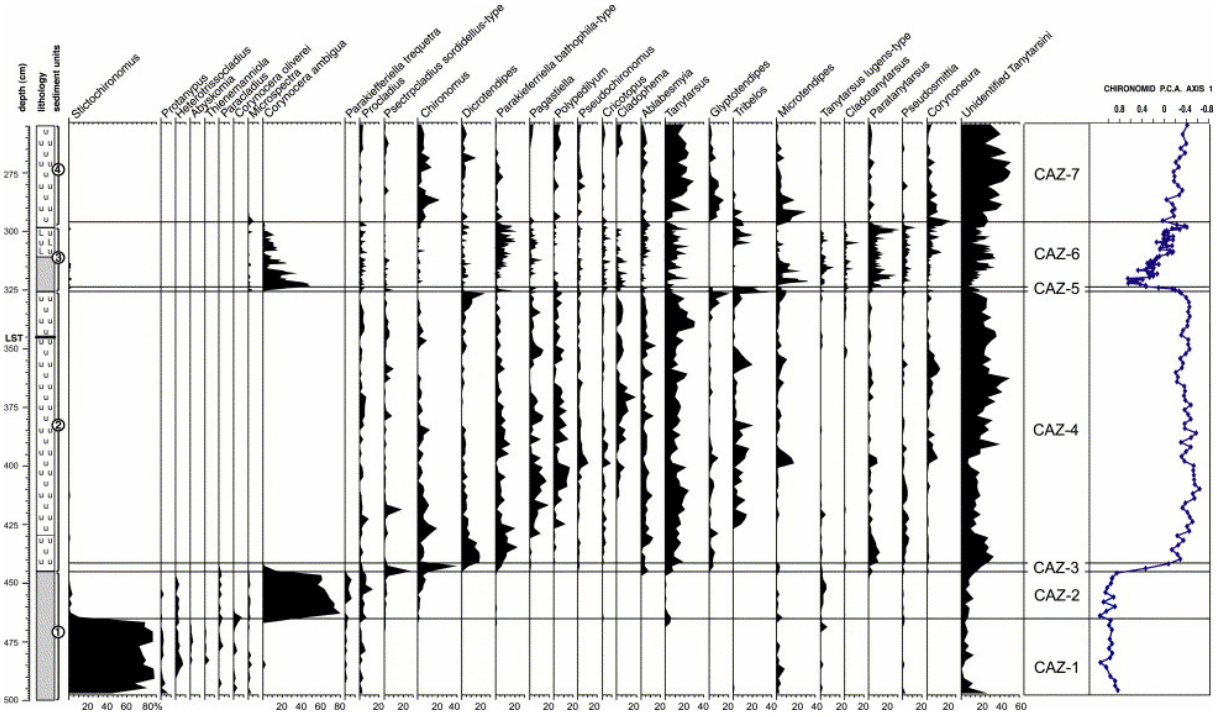

Fig. 5. Chironomid diagram from Lautrey core 6 (analysis: L. Millet). Chironomid PCA axis 1: see explanations in Section 12.2.

5.1. Laboratory methods

Samples for chironomid analysis were taken at 0.5 cm interval within the Younger Dryas pollen zone, while the sampling interval was increased to 2 cm for the rest of the sediment core. Chironomid head capsules were extracted from the sediment following the procedure described by Hofmann (1986). The amount of treated sediment per sample was adjusted to obtain about 100 head capsules as recommended by Heiri and Lotter (2001) and Larocque (2001). Identification of chironomid head capsules according to Hofmann (1971) and Wiederholm (1983) was performed, in most cases, at genus or species group level. The relative abundances of taxa were calculated for each sample from a sum of total chironomids to construct a percentage diagram.

5.2. The chironomid record

Seven chironomid assemblage zones (CAZs) have been distinguished. Palaeoecological interpretations were inferred from modern environmental preferences of taxa characterising the biozones.

In CAZ-1, the low taxa richness indicates strongly constraining environmental conditions. The zone is dominated by *Stictochironomus* associated with *Abiskomyia*, *Parakiefferiella triquetra*, *Heterotrissocladius*, *Paracladius*, *Monodiamesa* and *Protanypus*. These taxa are characteristic of oligo- to mesotrophic lakes in Saether's typology (1979) and are often found in well-oxygenated water (Quinlan and Smol, 2001).

The definition of zone CAZ-2 was mainly based on the dominance of *Corynocera ambigua*. The modern distribution and ecology of *C. ambigua* indicates that the species prefers water with large hydrophyte beds and high production of benthic diatoms (Brodersen and Lindegaard, 1999). The appearance of *Chironomus* and the higher relative abundance of *Procladius* suggest a slightly higher organic accumulation in the sediment probably associated with a decrease of oxygen concentrations.

During CAZ-3, *C. ambigua* declines, whereas the relative abundance of *Chironomus* and taxa richness sharply increase. CAZ-3 is only composed of two samples and must be considered a transitional zone between CAZ-2 and CAZ-4.

The onset of CAZ-4 corresponds to a strong change in the chironomid community. *C. ambigua* and all oxyphilous taxa characteristic for CAZ-1 and CAZ-2 disappear from the assemblages. The general characteristics of the zone are its high taxa richness and the high relative abundance of taxa, such as *Chironomus*, *Dicrotendipes*, *Polypedilum* and *Cladopelma*, often found in anoxic lakes. The higher taxonomic richness suggests a general improvement of environmental conditions allowing the development of a more diversified aquatic biota.

During CAZ-5, *C. ambigua*, one of the most characteristic taxa of the next zone CAZ-6, appears in the assemblages. *Tribelos* shows a sharp peak, but the ecology of this taxon is still poorly known. Hence, it is difficult to interpret this zone in terms of environmental conditions. Like CAZ-3, this very short-lived zone is considered a transitional phase.

Zone CAZ-6 displays an important change in the chironomid community. In general, there is a large re-expansion of *C. ambigua* (which had been absent since the end of zone CAZ-2), an increase in the relative abundance of *Microtendipes*, *Paratanytarsus* and *Tanytarsus lugens*, and the re-appearance of *Stictochironomus* and *Micropsectra*. The presence of *Microspectra*, *Stictochironomus* and *T. lugens* suggests an improvement of oxygen conditions, while the decrease in percentage of *Chironomus* and *Polypedilum* marks a reduction in organic accumulation. The relative abundance of *C. ambigua*, *Microtendipes* and *T. lugens* shows a downward trend in contrast with that of *Parakiefferiella bathophila*-type, *Ablabesmyia*, *Tribelos* and *Corynoneura*. This may indicate a progressive increase in pelagic production during the zone.

In zone CAZ-7, the assemblages are dominated by taxa living in muddy sediment (e.g. *Chironomus*) and able to survive long periods of anoxic conditions. The high relative abundance of *Glyptotendipes* suggests an expansion of aquatic vegetation.

6. Organic matter analysis

Several studies have demonstrated that OM preserved in lake sediments can provide information on regional environmental changes (Bertrand et al., 1992; Meyers and Lallier-Vergès, 1999; Bourdon et al., 2000). In a lake sediment sequence, OM originates from three major sources: (1) planktonic and benthic algae which may represent an important fraction of the total organic content in eutrophic waters, (2) submerged or emergent vascular plants which colonise the lake margins or the whole water-body during lowstands, and (3) terrestrial plant remains and soil OM removed by weathering from the catchment area.

6.1. Methods

Seventy-eight samples were taken from the core 6 for OM analysis with a focus on the phases of major climatic and environmental changes. Total organic carbon (TOC) content (wt% of dry sediment) was determined by Rock-Eval® pyrolysis with a model 6 device (Vinci Technologies; Espitalié et al., 1985). The analyses were carried out on 100 mg of crushed samples under standard conditions. Total N and C contents (wt%) were obtained with a LECO CNS 2000 Analyser. The C/N ratio is related to both the origin and the degree of degradation of total OM (Disnar et al., 2003).

The petrographic study (palynofacies) involves a microscopic examination of total OM, in transmitted and reflected light, after acid hydrolysis of carbonates and silicates. Taking into account the chromatic and textural aspects of particles (Sifeddine et al., 1998), the analysis aims at identifying and quantifying the organic compounds (relative percentages of surface particle area), and at establishing the ratio between allochthonous and autochthonous components. Terrestrial OM (TOM) includes particles weathered from the catchment and/or windblown grains, while lacustrine OM (LOM) consists of particles derived from aquatic plants and phytoplankton.

6.2. The organic matter record

TOC values fluctuate between 0.6% and 6.5% throughout the studied sequence (but which are mostly between 1.5% and 3%) and permit the distinction of four zones (Fig. 6). Increasing TOC values may reflect (1) an increase in the algal production, (2) a lake-level lowering and a correlative reinforcement of OM (derived) from marsh plants, and/or (3) larger inputs from the catchment (soils and plants). In all cases, the increase in OM sedimentation is expected to induce a decrease in dissolved oxygen and hence a better OM preservation. Thus, the C/N ratio (i.e. TOC/total N) which varies from 2.3 to 34.7 suggests important changes in the OM origin as well as in sedimentary conditions. Accordingly, high TOC and C/N ratio values like those recorded in OMZ 2c and 2e (Fig. 6) document increased inputs from rather well preserved vascular plant debris. In contrast, rather low C/N ratio values (usually between 4 and 10) such as those found in OMZ-3 can be taken as indicative of relatively higher importance of algal-derived OM. For the rest, most of the C/N values ranging between 10 and 15 suggest a mixed contribution from algae and vascular plants.

These general trends are supported by an estimate of the relative proportions of the TOC due to LOM and TOM (respectively; Fig. 6) based on TOC values and the relative proportions of organic debris from the lacustrine and terrestrial sources determined in the palynofacies assemblages. TOM mostly follows TOC; this suggests a dominant terrestrial origin of the OM inputs all along the sedimentary record, except for OMZ-1 (Oldest Dryas pollen zone) and OMZ-3 (Younger Dryas pollen zone) where lacustrine inputs might have been predominant.

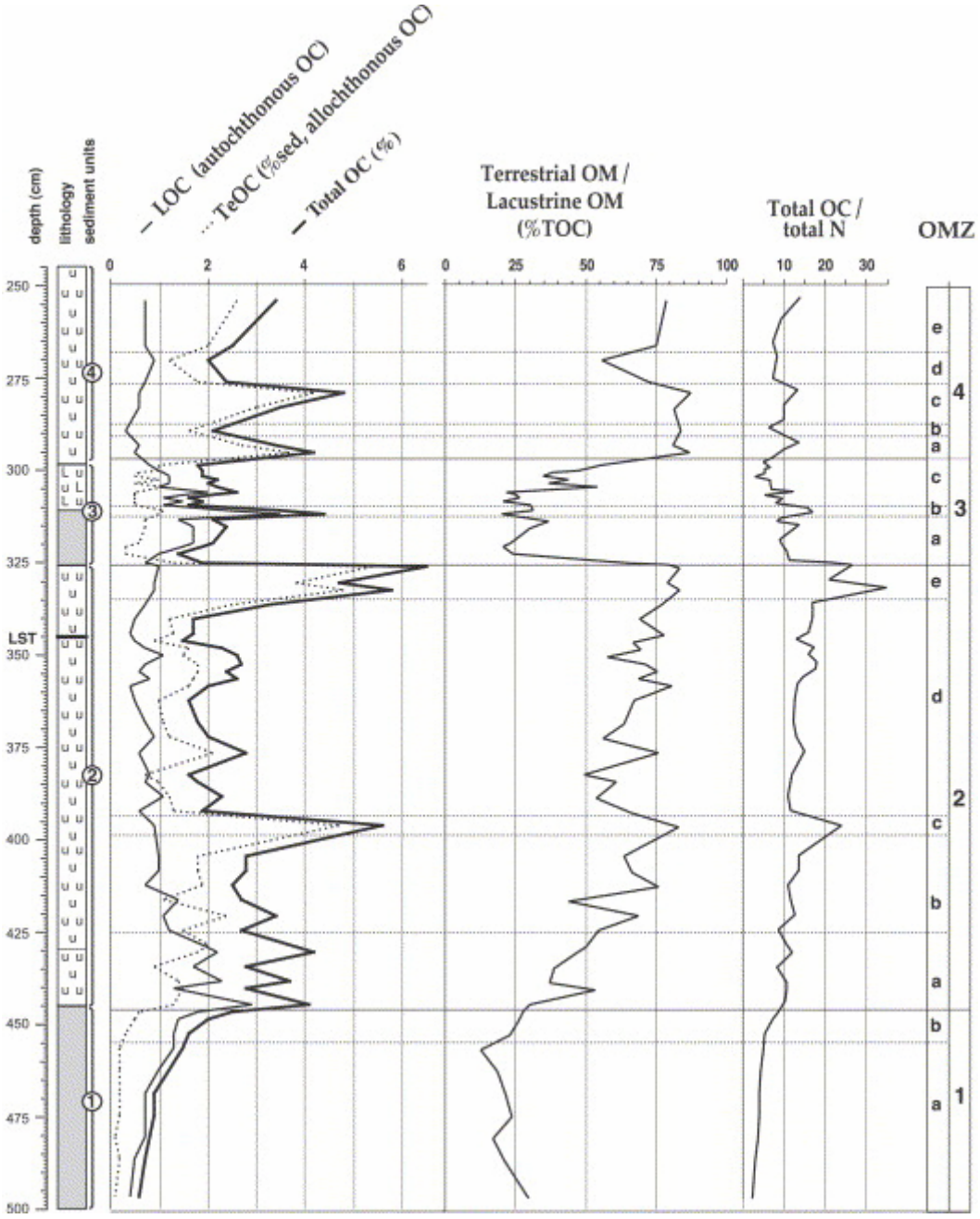

Fig. 6. Organic matter record from Lautrey core 6. TOM, terrestrial organic matter; TOC, total organic carbon; LOM, organic matter of lacustrine-autochthonous origin (in percentage of organic particle surface area in the palynofacies); LOC, organic carbon of autochthonous origin (in percentage of TOC following the equation: LOC=[TOC/100]×LOM); TeOC, organic carbon of allochthonous origin; OMZ, organic matter zones (analysis: B. Vannière).

The predominance of TOM in the studied section indicates that the OM sedimentation principally reflects the development of soils and vegetation on the paludal belt and in the catchment area.

7. Mineralogy and grain-size analysis

7.1. Methods

Samples for mineralogy and grain-size analysis were taken at 2 cm intervals from 250 to 497 cm depth. The grain size was measured by sieving. The bulk mineral composition was determined by X-ray diffraction, using an X'Pert Philips diffractometer with a cobalt anticathode. The diffractometer settings were 5 s per step from 3° to 72° 2θ for a bulk characterisation of non-oriented powdered samples (Holtzappfel, 1985). Given that samples reflect variable degrees of mineral mixing, the area of the major peak of each mineral was measured on the diffractograms. The semi-quantitative mineral composition was expressed as a percentage (Moore and Reynolds, 1997; Amorosi et al., 2002). The Rcm ratio indicates the variations in the occurrence of clay minerals in the sediment (Rcm=[(sum of peak areas of the clay minerals)×100]/[sum of the peak areas of all minerals]). The relative occurrence of illite, kaolinite and chlorite was estimated by comparing with the principal peak of the dominant mineral (quartz or calcite) on the diffractograms.

In addition, further mineralogical observations were carried out on samples characterised by MS peaks (see Section 8) at levels 345, 348.5 and 352.5 cm, which were assumed to contain ash layers. These samples were divided into three subsamples and etched by HCl 0.5 N for carbonate dissolution and filtered. The insoluble residue was air-dried. The first and the second subsamples were observed, respectively, under a photonic microscope after setting in epoxy resin and polishing, and under a scanning electron microscope (Jeol 5600 with X-EDS Fondis-99 microanalysis). The third subsample was analysed by X-ray diffraction for the detemination of magmatic and neoformed minerals. These samples were prepared following the procedure of Kubler (1987). Each powdered residue was analysed using a SCINTAG XRD 2000 diffractometer running between 2° and 65° 2θ at 45 kV and 40 mA using Cu Kα radiation and a scan speed of 1°/min.

7.2. The mineralogy and grain-size records

Quartz and calcite are the main minerals with feldspars (mainly plagioclase) and clay minerals (illite, kaolinite, chlorite and rare smectites) as accessory minerals. Dolomite, jadeite (pyroxene) and sanidine (K-feldspar) are observed occasionally. Five zones (MZ) have been distinguished as follows (Fig. 7).

MZ-1 (500–445 cm) is characterised by (1) the predominance of quartz and the presence of feldspars, (2) low values of calcite, and (3) an important amount of clay minerals. Quartz appears as silty grains with wind abrasion marks, which suggest long-distance transport. Given the quasi-absence of biogenic calcite, the MZ-1 deposits correspond to detrital sedimentation as a result from erosion in the catchment area and long-distance transport. The importance of the wind is also illustrated by the presence of exogenic clay minerals, such as illite and chlorite. Above 475–470 cm depth, the decrease in Rcm as well as the weakening and subsequent disappearance of kaolinite reflect a weakening of mineral sources and/or wind strength.

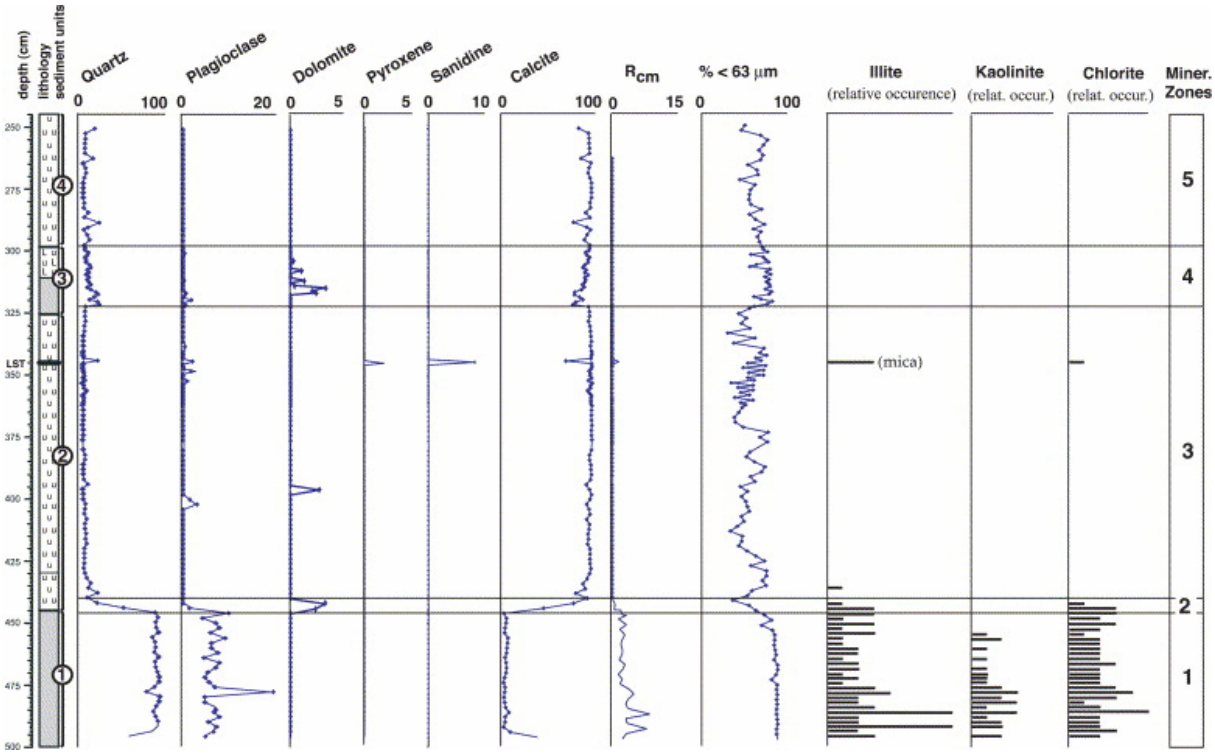

Fig. 7. Grain size (by sieving) and mineralogy record from Lautrey core 6 (analysis: A.V. Walter-Simonnet).

MZ-2 (445–440 cm) is marked by a rapid decrease in quartz and plagioclase, a correlative increase in calcite, a quasi-disappearance of illite and chlorite, and a narrow peak in dolomite. It reflects warmer climatic conditions with the transition from accumulation of allochthonous detrital input to formation of biogenic carbonate deposits in the lake basin.

MZ-3 (440–322 cm) is characterised by high, relatively constant values of calcite. Regarding the grain size, the <63 µm fraction shows values generally lower and more variable than in MZ-1. Short-lived peaks of plagioclase (at level 402 cm) and dolomite (at level 396.5 cm) may be related to erosion of some specific, limited parts of the catchment area.

Analyses indicate that the three successive peaks in MS at levels 345, 348.5 (Laut 1) and 352.5 cm (Laut 2) correspond to samples containing volcanic glass shards and magmatic minerals as well as calcite, quartz and clay minerals. On the basis of petrographic and SEM observations, the mineral composition of these tephra layers has been extensively described in Vanniere et al. (2004). Sample 345 cm corresponds to the LST as classically observed in other European sites (van der Bogaard and Schmincke, 1985), whereas the mineral composition of the LAUT 1 and LAUT 2 horizons suggests a trachytic volcanism similar to the Chaîne des Puys volcanoes in the Massif Central (France), where two tephras from Le Puy de la Nugère have been dated by Juvigné et al. (1996) and Vernet and Raynal (2000) to 12,010±150 and 11,360±130 ^{14}C yr BP (Vanniere et al., 2004).

The beginning of MZ-4 (325–298 cm) is marked by a minor decrease in calcite and a rapid increase in the <63 µm fraction and in quartz, plagioclase and dolomite. This indicates a reactivation of the detrital input inherited from long-distance transport (quartz) and erosion processes in the catchment area (dolomite), as well as a weakening of autochthonous sedimentation of biogenic carbonate. All these point to a cool and windy period. The later part

of MZ-4 shows a progressive recovery of the biogenic sedimentation correlative with a reduction of detrital input.

During MZ-5, the calcite quasi-exclusively dominates the sedimentation apart from some minor peaks of quartz.

8. Magnetic susceptibility measurements

MS measurements have proved to be a useful guide for the detection of environmental changes (Thouveny et al., 1994; Stockhausen and Zolitschka, 1999). Erosion, soil processes in the catchment area and lake productivity can result in different assemblages of magnetic minerals in lake sediment sequences. Previous work in carbonate lakes in England and France have shown that MS maxima may reflect intense detrital events in response to (1) climate cooling and changes in vegetation cover during the Lateglacial period (Nolan et al., 1999), or (2) forest clearings and land use history (Higgitt et al., 1991). Volume MS depends mainly on magnetite concentration in sediments. Nevertheless, in the case of low concentration of ferrimagnetic minerals, the MS values can be largely influenced by diamagnetic minerals, such as quartz and carbonate (Thompson and Oldfield, 1986).

8.1. Methods

The volume MS was measured using the MS2E1 surface scanning sensor (Nowaczyk, 2001). This sensor of high sensitivity and small spatial resolution is well suited for measuring MS of split cores at a high resolution. The measurements were systematically carried out at 0.5 cm intervals with a sensitivity of 0.1×10^{-8} SI.

8.2. The MS record

Five MS zones can be distinguished from the MS record of core 6 as follows (Fig. 8).

MSZ-1 corresponds to sediment unit 1 and is characterised by high MS values. Subzone MSZ-1a shows higher values than subzone MSZ-1b. Subzone MSZ-1c is a transitional zone with a rapid fall in the MS values. MSZ-2 displays a general trend towards low values interrupted by minor maximums at levels 440–424, 428–425 and 419–415 cm. In MSZ-3, MS values show a relatively constant and low level except for samples 355–342 cm, where higher values are associated with three tephra layers (see Section 7), and for samples 333–326 cm, where a slight increase is observed. MSZ-4 is marked by a rapid increase in MS values followed by a progressive decline affected by a short-lived minimum at level 310 cm. A rapid fall in MS values occurs between samples 301 and 298 cm. MSZ-5 (Preboreal pollen zone) indicates a recovery of values prevailing during MSZ-3, followed by a general trend towards weakening.

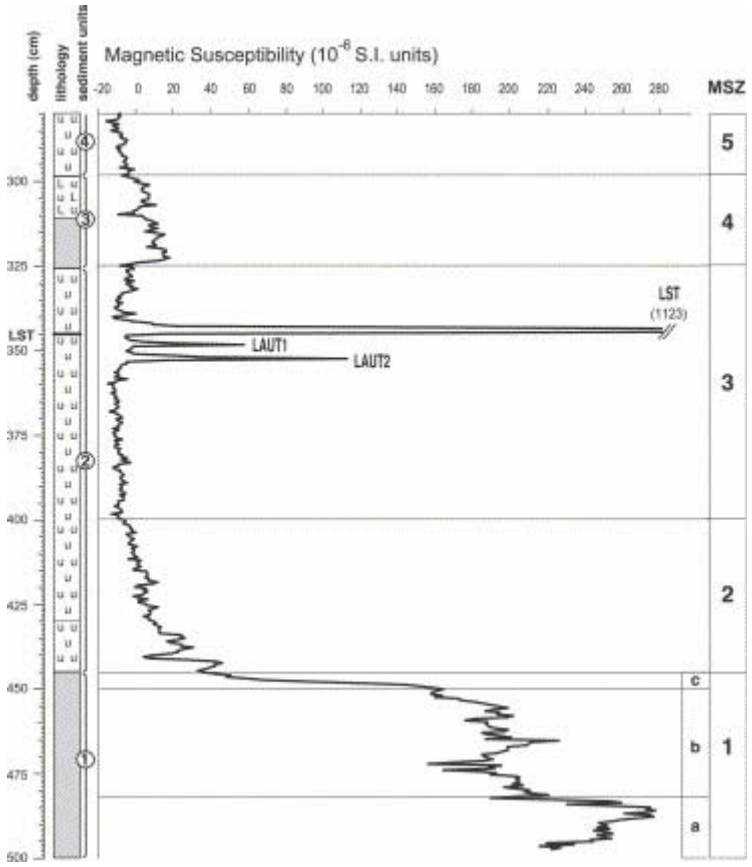

Fig. 8. Magnetic susceptibility record from Lautrey core 6 (analysis: G. Bossuet and B. Vannière).

Generally speaking, a correspondence is apparent between higher MS values and sediment units 1 and 3 characterised by a large proportion of allochthonous minerogenic deposits, whereas sediment units 2 and 4 marked by biogenic carbonate formation in the lake coincide with lower MS values. Moreover, it is noteworthy that even during the deposition of minerogenic sediment unit 3, MS values never reach the maximal values characteristic for MSZ-1a and MSZ-1b. In addition to the mineralogy data, this suggests a mixture of allochthonous and autochthonous sediments.

9. Oxygen-isotope analysis

9.1. Method

The shifts in oxygen-isotope ratio measured in precipitated lake carbonates are generally assumed to reflect climate changes without any lag. It is hypothesised that the isotopic composition depends only on the ratios in the atmospheric water vapour and the temperature. However, as noted by Ammann et al. (2000), three weaknesses may affect this basic assumption as follows:

• Detrital or reworked carbonates may alter or distort the climatic signal.

• Variations in isotopic ratios caused by changes in moisture origin may be difficult to separate from changes due to temperature.

• Hydrological changes reflected by lake-level fluctuations may also be responsible for changes in isotopic ratios.

However, Lotter et al. (1992) have shown that not only major shifts in the oxygen-isotope profiles obtained from analysis of bulk carbonate in Swiss lakes, but also minor shifts can be compared with equivalent features recognised in the Greenland oxygen-isotope record. Moreover, similar oxygen-isotope records obtained from bulk carbonate samples have been established for the Last Glacial–Interglacial transition from several Jura lake sediment sequences (Eicher, 1987; Magny, 1995; Aalbersberg et al., 1999).

The development of an oxygen-isotope profile for Lautrey core 6 was considered important in order to generate a direct record of climate changes that is independent from biotic and abiotic proxies. It is then possible to evaluate the response of ecosystems to climatic variations. A second objective was to derive an indirect time-scale for the sequence by correlating the ^{18}O record with that of the GRIP ice core, as discussed below (see Section 12.1).

Bulk sediment samples for measurements of the $^{18}O/^{16}O$ ratio were analysed at 0.5 cm intervals for the section spanning the Younger Dryas pollen zone and at 1 cm intervals for the rest of the sediment core. Care was taken that the analysed samples consisted entirely of carbonate, with no shell fragments. Oxygen-isotope ratios were analysed on a Finnigan MAT 252 mass spectrometer equipped with an automated carbonate extraction line. Samples were digested in concentrated orthophosphoric acid at a temperature of 80 °C. All data are reported relative to the V-PDB standard.

9.2. The oxygen-isotope record

The large fluctuations in values below level 445 cm in the Oldest Dryas pollen zone clearly show that the climatic signal was strongly perturbed by effects of old carbonate lithoclasts originating from the Jurassic and Cretaceous rocks in the catchment area. The occurrence of clay minerals, quartz, dolomite and lithoclasts illustrated in Fig. 7 and Fig. 10 suggests possible perturbations of the climatic signal provided by the oxygen-isotope record during the Lateglacial Interstadial and the Younger Dryas pollen zone. Nevertheless, the isotopic profile reconstructed above 445 cm depth generally shows a rather coherent picture (Fig. 9).

The oxygen-isotope profile of core 6 presents two well-marked maxima. The first between 445 and 435 cm occurs at ca 12,590±45 ^{14}C yr BP and coincides with the beginning of Bølling–Allerød pollen zone. The second, at 295 cm depth, is dated to 10,000 ^{14}C yr BP and corresponds to the beginning of the Holocene. These two maxima reach similar levels of isotopic values and reflect important warming phases.

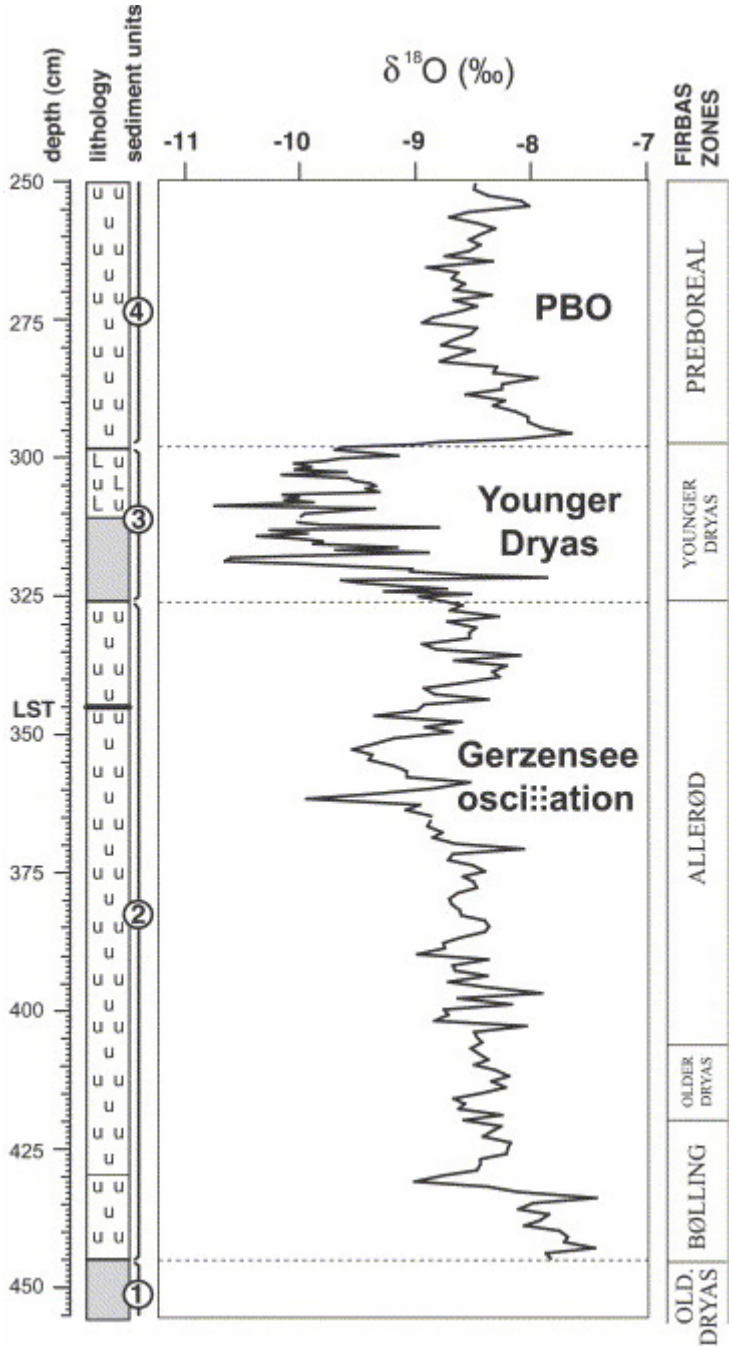

Fig. 9. Oxygen-isotope record from Lautrey core 6 (analysis: G. Aalbersberg).

Another prominent feature is the long-lasting minimum which culminates between 326 and 298 cm depth. It develops between 10,960±45 and 10,000±40 ^{14}C yr BP and corresponds to the Younger Dryas pollen zone. The end of this cold event shows an abrupt increase in $^{18}O/^{16}O$ ratio as is also observed in the Gerzensee and GRIP oxygen-isotope records (Johnsen et al., 1992). However, in contrast to the classical characteristics of the onset of the Younger Dryas pollen zone in these records, the isotopic profile of Lautrey core 6 does not present a rapid decrease in isotopic values at that time, even though the lithostratigraphy indicates a sharp transition at level 326 cm from carbonate lake-marl to clayey-silty deposits. The abrupt input of lithoclasts from the catchment area at the Younger Dryas onset (see Section 10, Fig.

10) was probably responsible for perturbations of the isotopic signal. Furthermore, the oxygen-isotope signal during the Younger Dryas biozone shows rapid and strong (>2‰) fluctuations, equally attributable to the presence of allochthonous material.

Shortly after the beginning of the Holocene, a less pronounced minimum develops between 284 and 266 cm depth, i.e. between 10,120±40 and 9975±45 ^{14}C yr BP and corresponds to the Preboreal oscillation (PBO) (Lotter et al., 1992; Björck et al., 1997). It was preceded by a short-lived minimum at level 289 cm.

Two other minima appear between levels 363 and 352 cm. They occur after 11,575±45 ^{14}C BP and immediately precede the deposition of LST. These events can be attributed to the Gerzensee oscillation (Lotter et al., 1992; Björck et al., 1998). As noted by Schwander et al. (2000), the magnitude of the isotope signal during the Gerzensee oscillation and PBO reaches about one-third to one-half of the magnitude of the big shifts at the Bølling and Holocene onsets.

Before the Gerzensee oscillation, no particularly prominent event can be recognised except from that culminating at level 430 cm, i.e. inside of the Bølling pollen zone. No major climate cooling in the isotope profile of Lautrey core 6 can be observed between 419 and 404 cm depth, i.e. at the time of the Older Dryas pollen zone (see Section 4). Detrital inputs from the catchment area can be suspected to have perturbed the isotope signal as suggested, e.g., by a peak of lithoclasts in the fraction <63 μm between levels 420 and 415 cm (see Section 10, Fig. 10).

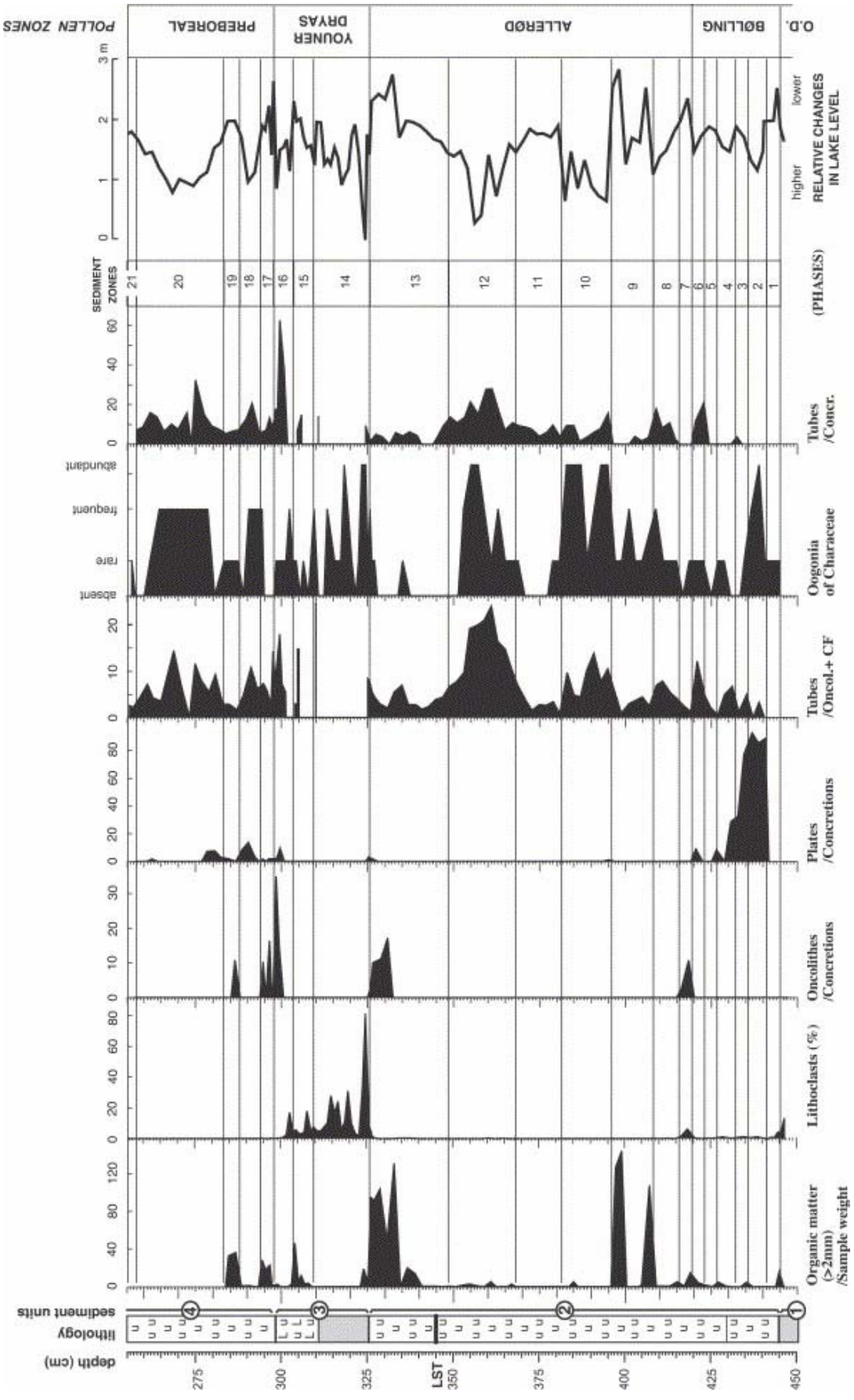

Fig. 10. Sediment diagram and lake-level record from Lautrey core 6 (analysis: M. Magny).

10. Lake-level reconstruction

Lake-level reconstructions for the Lateglacial period provide useful proxy palaeoclimatic data for continental areas (Gaillard and Moulin, 1989; Bohncke and Vandenberghe, 1991) and high-resolution studies have shown an in-phase behaviour between lake-level and isotope signals (Magny, 2001).

10.1. Methods

The reconstruction of past changes in lake level for the Lautrey core 6 is based on a particular sedimentological approach which uses a combination of several markers and comparisons with modern analogues observed in sediments in present-day lakes (Magny, 1992a, Magny, 1992b and Magny, 1998) as follows:

• *Lithological criteria*: Littoral sediments are often characterised by a larger quantity of OM originating from shore vegetation than open water parts of the lake. Fine carbonate lake-marl is deposited in deeper water.

• *The macroscopic components of lake marl*: The coarser fractions (larger than 0.2 mm) of lake-marl accumulated in the Jura lakes are mainly composed of carbonate concretions of biochemical origin (Magny, 1992a, Magny, 1992b and Magny, 1998). These concretions can be divided into several morphotypes. Modern analogues based on surface samples taken along transects perpendicular to the shore have revealed, that each morphotype shows a characteristic spatial distribution from the shore to the profundal zone reflecting both the hydrodynamics and aquatic vegetation belts. Oncolithes characterise near-shore areas; cauliflower-like forms dominate the littoral platform, plate-like and tube-like forms develop on the edge and slope of the littoral platform and are associated with *Nuphar-Potamogeton*- and Characeae belts, respectively.

10.2. The lake-level record

Table 2 provides a summarised description of the 21 successive local sediment zones (SZ) distinguished from the sedimentological analysis of Lautrey core 6 (Fig. 10). The quasi-absence of biogenic carbonate concretions below 445 cm depth did not permit the establishment of a lake-level record from sediment unit 1.

Table 2. : Lateglacial and early Holocene lake-level changes reconstructed from Lautrey core 6

Zones/phases	Lake level	Main sedimentological markers
21	Lower	Decrease in tube concretions and Characeae oogones
20	Higher	Peak of tube concretions and Characeae oogones
19	Lower	Peak of oncolithes
18	Higher	Peaks of plate and tube concretions, and oogone maximum
17	Lower	Peak of oncolithes, maximum of organic matter
16	Higher	Peaks of plate and tube concretions, and oogone maximum
15	Lower	Peak of organic matter, decrease in Characeae oogones
14	Higher	Peaks of lithoclasts and Characeae oogones
13	Lower	Peaks of organic matter and oncolithes, decrease in tube concretions and Characeae oogones
12	Higher	Peaks of tube concretions and Characeae oogones
11	Lower	Decrease in tube concretions and Characeae oogones
10	Higher	Peaks of tube concretions and Characeae oogones
9	Lower	Bipartited phase: peak of organic matter, decrease in tube concretions and Characeae oogones
8	Higher	Peaks of tube concretions and Characeae oogones
7	Lower	Peaks of organic matter and oncolithes
6	Higher	Peak of tube concretions
5	Lower	Small peak of organic matter, decrease in tube concretions
4	Higher	Peak of tube concretions
3	Lower	Small peak of organic matter, decrease in plate concretions and Characeae oogones
2	Higher	Peaks of plate concretions and Characeae oogones
1	Lower	Peak of organic matter, decrease in lithoclasts

SZ1 corresponds to a rapid fall in lake level at the transition between the Oldest Dryas and Bølling pollen zones. Rather unstable lake-level conditions characterise SZ-2 to 9. Two more pronounced maxima appear centred at levels 438 and 410 cm, and two marked lowering phases at 406 and 398 cm depth, as shown by the large amount of coarse OM inherited from the near-shore areas.

SZ-10 and 12 represent two major lake-level maxima. Each was followed by a well-developed phase of lower water level (SZ-11 and 13). During the latter part of SZ-13, peaks of OM and oncolithes reflect a major lowering.

The beginning of the Younger Dryas pollen zone is marked by a rapid rise in lake-level culminating at 324 cm depth (SZ-14). A general trend towards lowering can be recognised over the stadial period.

The onset of the Holocene corresponds to a rapid fall in water level (SZ-17) followed by two successive phases of higher lake level, a first short-lived (SZ-18) and a second more prolonged (SZ-20).

Generally speaking, the pattern of hydrological changes reconstructed at Lautrey corresponds well with lake-level records reported in previous studies of sites in west-central Europe (Magny, 2001).

11. Quantitative reconstructions of climatic parameters

With the exception of isotope studies, most of the quantitative reconstructions of palaeoclimates from Europe and North America until now have been obtained from coleopteran, cladoceran, chironomid and pollen-assemblage data. Coleoptera and chironomid-assemblage data primarily provide temperature reconstructions, whereas pollen data may provide information on both temperature and precipitation. Lake-level data offer an additional constraint to refine the modern analogue approach developed for pollen data (Guiot et al., 1993; Magny et al., 2001). Moreover, the quantitative reconstructions based on coleopteran, chironomid and pollen data provide only indirect palaeoclimatic inferences based on the response of plant and animal communities to climate changes. This response may also have been modulated by multiple non-climatic factors, such as the specific sensitivity of different organisms, edaphic conditions, colonisation and immigration processes and, more generally speaking, complex interactions between biota in ecosystems (van Geel, 1996; Hoek, 2001). The project initiated at Lake Lautrey offers the opportunity of a comparison of quantitative palaeoclimatic reconstructions based on biological climate indicators. The results are presented in Fig. 11 and discussed in Sections 12 and 13.

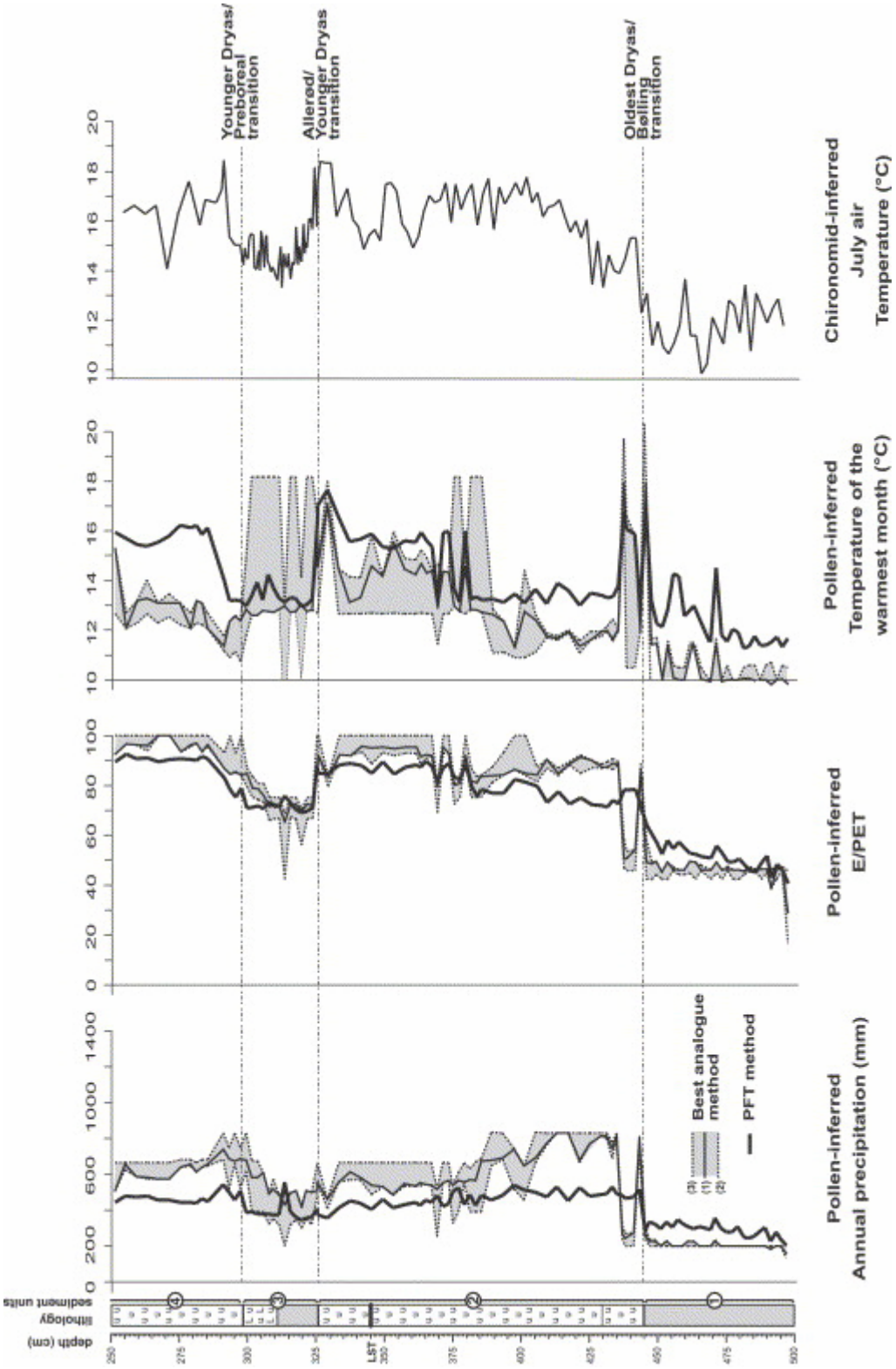

Fig. 11. Pollen- and chironomid-based quantitative reconstructions of climatic parameters from Lautrey core 6 (analysis: O. Peyron, O. Heiri and L. Millet). The curves reconstructed from the best analogue method show (1) the mean value calculated over the analogues, (2) the mean minimum and (3) the mean maximum values.

11.1. Pollen-based reconstruction

To provide more accurate and reliable palaeoclimatic estimates, two independent methods have been used as follows. In the "Best Analogue method" (BAM), the similarity between fossil and modern pollen assemblages is evaluated (Guiot, 1990). The modern spectra which have the smallest chord distance to given fossil assemblages are considered the best modern analogues, and used for the reconstruction of palaeoclimate. For each fossil pollen assemblage, the 10 best analogues are selected; consequently, their climatic parameters are averaged to provide the climate estimates. Furthermore, the best analogues selection is constrained by biomes and lake levels (Guiot et al., 1993; Magny et al., 2001).

The plant functional types (PFTs) method is a transfer function in which pollen percentages are first transformed into PFT scores (Peyron et al., 1998). PFTs are broad classes of plants defined by their structural and functional features (Prentice et al., 1996). The principle of the method is that PFT scores derived from the modern pollen samples are calibrated in terms of climatic parameters, using a non-linear regression method (artificial neural network). Then, the calibration is applied to the fossil PFT scores to provide the climate estimates.

The modern pollen data set used in the quantitative reconstructions includes 868 surface pollen samples from Eurasia including the Mediterranean basin, Pyrenees, Scandes Mountains, Kazakhstan and the Tibetan plateau (Peyron et al., 1998) to get samples more representative of some specific past vegetation types. Table 3 presents the correlation coefficients between observed and reconstructed values of climate parameters. The standard best modern analogue method and the PFT method, based on groups of pollen taxa, have been tested and compared to reconstructed mid-Holocene past climate. Although both methods indicate similar climatic patterns, the PFT method provides more consistent results (Peyron et al., 2000). On the basis of modern pollen data set coupled with known climatic conditions, the climatic parameters (i.e. the mean temperature of the warmest month, the annual precipitation and the ratio of real to potential evapotranspiration: E/PET) have been calculated using an artificial neural network calibration (Harrison et al., 1993; Peyron et al., 1998). The validation tests (Table 3) may suggest that the BAM reconstructions are more accurate than the PFT method. In theory, the artificial neural networks used in the calibration are able to learn and reproduce any pattern perfectly. However, if the network is fitted too closely to the input data, there is a risk that estimates of new data will be incorrect. Consequently, even if the correlation coefficients are lower with the PFT method than with the MAT, we consider the calibration procedure to be optimal because the relationships between the input and the output variables are learnt in a generalised fashion and can therefore be used for predictions of unknown outputs.

Table 3. : Correlation coefficients between observed and reconstructed values of climate parameters obtained from application of both modern analogue technique (MAT) and plant functional types (PFT) approaches to the modern pollen samples

Climatic parameter	**Best analogues method**		**Plant functional types method**		
	Correlation coefficient (r^2)	**RMSE**	**Correlation coefficient for the calibration**	**Correlation coefficient for the verification**	**RMSE**
Temperature of the warmest month (°C)	0.94	2.0	0.88±0.016	0.87±0.020	3.1
Annual precipitation (mm)	0.90	162	0.81±0.014	0.80±0.030	212
Ratio of real to potential evapotranspiration (%)	0.94	9.8	0.91±0.007	0.90±0.012	13.3

Note: In the PFT method, the original data set has been divided into training and verification sets. The artificial neural network is calibrated on samples from the training set. Samples of the verification set are used to verify the prediction of the climatic parameters. Samples included in both sets correspond to data randomly extracted in the modern data set. This procedure has been repeated to reach 30 simulations using bootstrap technique. Coefficients of correlation and standard deviation after the calibration and the verification have been calculated. Root mean square error (RMSE) is also indicated.

11.2. Chironomid-based reconstructions

Recently, there is an increasing interest in subfossil chironomid assemblages to establish quantitative records of past changes in summer temperature. Several models have been developed (Lotter et al., 1997; Olander et al., 1999; Brooks and Birks, 2000) which measure the relationship between the present-day summer temperatures and chironomid assemblages in surficial lake sediments. The chironomid-based July air temperature record presented in Fig. 11 was reconstructed from a chironomid-temperature inference model based on a modern training set from the Jura mountains, Swiss Plateau and Swiss Alps (Heiri, 2001; Heiri et al., 2003a). The transfer function is based on weighted averaging-partial least-squares regression and has a leave-one-out-cross-validated coefficient of determination (r^2) of 0.80, and a root mean square error of prediction of 1.53 °C for July air temperature.

During two intervals of the Lake Lautrey record, chironomid assemblages are dominated by taxa not present in surface sediment assemblages used to calibrate the transfer function. This non-analogue situation was mainly due to the occurrence of *C. ambigua* and to *Pagastiella*. As a consequence, temperature inferences from samples with a high proportion of *C. ambigua* and *Pagastiella* (CAZ-2 and the oldest part of CAZ-6) are based on only a part of the chironomid fauna and on a comparatively lower number of chironomid specimens. As discussed by Heiri and Millet (2005), this implies that inferred temperatures at the end of the Oldest Dryas and at the beginning of the Younger Dryas pollen zones should be interpreted with caution, as they are based on samples with a high proportion of *C. ambigua* and *Pagastiella*. Moreover, the Lake Lautrey sediment sequence represents sublittoral/littoral deposits and Millet et al. (2003) have suggested that the chironomid record of Lake Lautrey may also reflect changes in trophic and oxygen conditions in addition to changes in substratum. Recent studies indicate that a bias in inferred temperatures is possible if chironomid-temperature inference models calibrated on deep-water sediments are applied to

near-shore assemblages (Heiri et al., 2003b). In lakes of a similar water depth as the Lake Lautrey palaeolake, this bias has been estimated to be of ca 0.4–0.5 °C magnitude and is therefore relatively small in comparison with the Lateglacial temperature changes inferred for the Lake Lautrey record (Fig. 11).

12. Synthesis of environmental and climatic changes

Taken together, the records presented above offer a basis for a tentative synthesis of environmental and climatic changes at Lake Lautrey during the Last Glacial–Interglacial transition. However, in order to evaluate the rapidity of changes and possible lags and offsets in biotic and abiotic responses to climate variations, it is necessary to estimate the sampling resolution of these records by establishing an absolute calibrated time-scale.

12.1. Construction of an age-depth model

Fig. 12 presents the strategy used to construct an age-depth model for Lautrey core 6. It results from the combination of tephra, radiocarbon and isotope data described in the previous sections.

First, the LST horizon offers a useful time-marker dated to ca 12,850 cal yr BP (see Section 3).

Second, 12 AMS radiocarbon dates provide a time framework (Fig. 12B, Table 1 in Section 3) fully consistent with the pollen and isotope stratigraphy available for the Jura mountains region (de Beaulieu et al., 1994; Magny, 1995; Bégeot, 2000) and more generally, for west-central Europe (Ammann and Lotter, 1989; Lotter et al., 1992; Brauer et al., 1999). However, when attempting to produce an absolute time-scale, difficulties appear due to the uncertainties associated with (1) the size of the time windows given by the calibration of the radiocarbon ages, and (2) periods of near-constant ^{14}C age at ca 12,700–12,600 and 10,000–9900 cal yr BP (Lowe et al., 1999). We have also to keep in mind that the calibration back to 12,600 $\partial^{14}C$ in IntCal 1998 is still not fully reliable.

By direct comparison with the GRIP ice-core isotope record, the oxygen-isotope record obtained from Lautrey core 6 provides the possibility to overcome the difficulties mentioned above. A similar strategy was used previously (Grafenstein et al., 1999; Ammann et al., 2000) with the basic assumption that the shifts in ^{18}O record reflects air mass changes and climatic variations without any lag. As illustrated by Fig. 1, Lake Lautrey is located close to the sites of Gerzensee (Swiss Plateau), Meerfelder Maar and Ammersee (Germany) where a quasi-synchronicity has been observed between climatic events recorded in the Greenland ice-sheet and those reconstructed in west-central Europe, based on (1) varved sediments (Brauer et al., 2000), (2) a comparison between oxygen-isotope records (Grafenstein et al., 1999; Ammann et al., 2000), or (3) a combination of oxygen-isotope and pollen stratigraphies (Lotter et al., 1992). Keeping the disturbance of the isotopic signal at Lautrey due to detrital inputs at the beginning of Younger Dryas biozone and during the Older Dryas oscillation in mind (see Fig. 6, Fig. 7 and Fig. 10), the correlations presented in Fig. 12 show a reasonable agreement between the Lautrey and GRIP isotopic records.

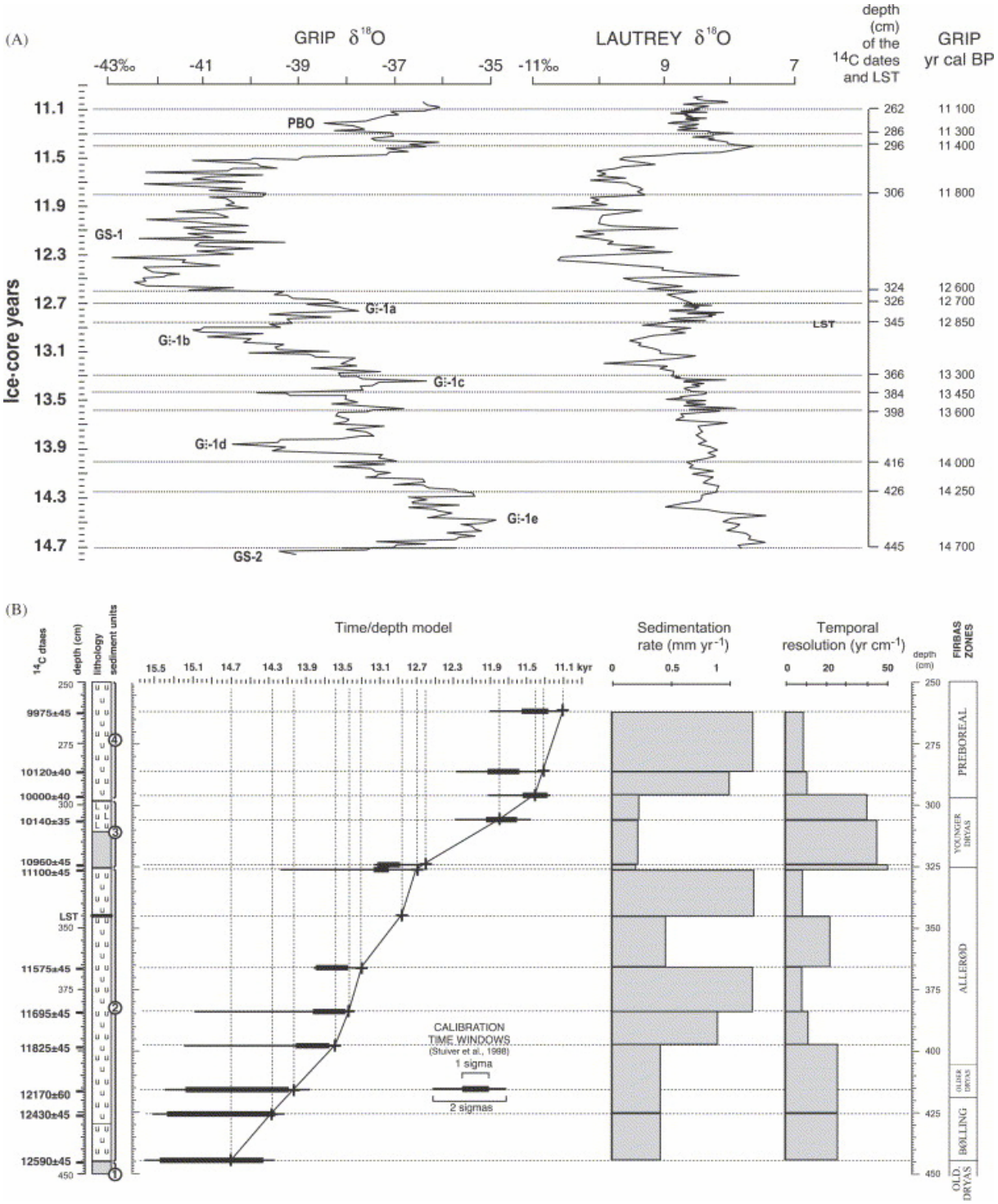

Fig. 12. Correlation between the ^{18}O record of Lautrey core 6 and that of GRIP ice core (A), within the constraints imposed by the age of LST and the limits of the time windows given by the calibration of the radiocarbon dates as shown in B. The points marked by + correspond to chosen time inside the time window given by the calibration according to a comparison of the Lautrey oxygen-isotope record with that of the GRIP record (Johnsen et al., 1992) rather than to the probability distributions. The inferred sedimentation rate and corresponding temporal resolution for, as an example, a 1 cm sampling interval, are indicated in B. Due to disturbances of the Lautrey oxygen-isotope record by detrital input at the Oldest Dryas–Bølling and the Allerød–Younger Dryas transitions, the abrupt changes in the lithology at levels 445 and 326 cm have been chosen to place the GS-2/GI-1e and GI-1a/GS-1 transitions. This is consistent with the pollen and chironomid stratigraphies.

Thus, on the basis of a general similarity between the GRIP and Lautrey oxygen-isotope records (see Section 9) and taking into account the limits of the time windows given by the calibration (intercept method in IntCal 4.3, Stuiver et al., 1998), each of the 12 levels radiocarbon dated at Lautrey has been correlated with a level of the GRIP record (tuning by wiggle matching between GRIP and Lautrey oxygen-isotope records). The LST horizon provided an additional time linkage. In between the intervals defined by LST and the radiocarbon dated levels, no further tuning by wiggle matching has been done, but a mean sedimentation rate has been calculated for each interval as illustrated in Fig. 12. This sedimentation rate allows the estimation of the variations in the time resolution reached by the samples from the different segments of the Lautrey core 6. Due to disturbances of the Lautrey oxygen-isotope record by detrital input at the Oldest Dryas–Bølling and the Allerød–Younger Dryas transitions, the abrupt changes in lithology at levels 445 and 326 cm have been chosen to determine the positions of the GS-2/GI-1e and GI-1a/GS-1 transitions. This is consistent with the pollen stratigraphy.

12.2. Environmental evolution and climatic history

For the pollen and chironomid biostratigraphical data sets, detrented correspondence analysis (DCA) was used to measure the gradient length of the first principal components analysis (PCA) axis in Standard Deviation units (Ter Braak and Smilauer, 1998). This resulted in a gradient length lower than 4 for both the data sets, justifying the further use of the linear response model and hence of PCA. In PCA, percentage of pollen and chironomid data were log-transformed ($Y'=\log[Y\times1+1]$) and centred on species. According to PCA, the first axis explains, respectively, 56% and 23% of the variation of pollen and chironomid data sets, respectively. All ordinations were implemented using the CANOCO program for Windows 4.0 (Ter Braak and Smilauer, 1998).

In order to make the comparison with other data more objective, the more complex pollen and chironomid data are presented in Figs. 13 (Oldest Dryas biozone) and 14 (Bølling–Allerød biozones and Holocene) using curves defined by the scores of PCA axis 1. As illustrated by Fig. 4, the pollen PCA axis 1 mainly reflects the AP/NAP curve, i.e. below 405 cm primarily the *Betula* and above this level primarily the *Pinus* percentages. Fig. 5 shows that the chironomid PCA axis 1 appears to mirror chiefly the percentages of *C. ambigua* and *Stictochironomus*.

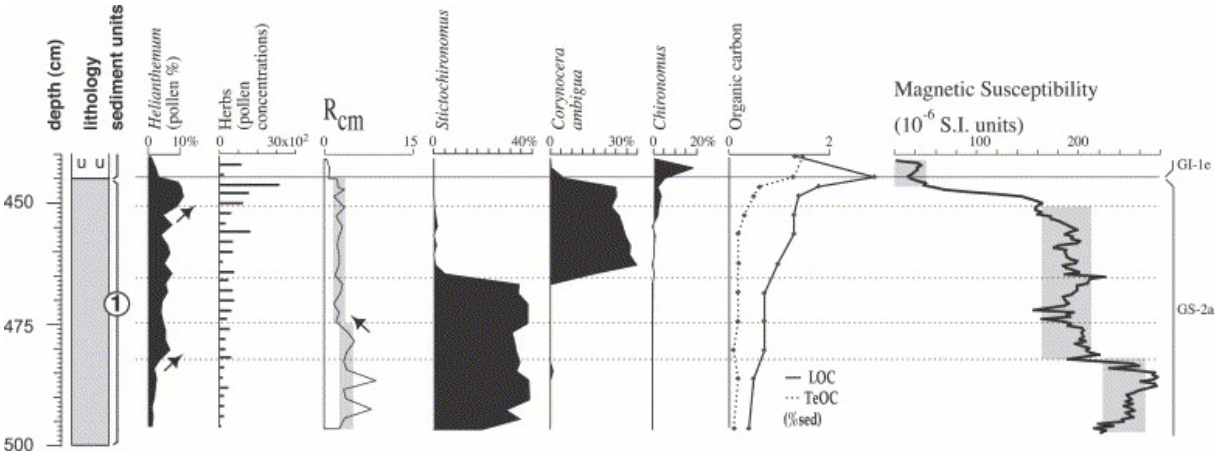

Fig. 13. Environmental synthesis for the Greenland Stadial 2a as documented by Lautrey core 6.

12.2.1. Sediment unit 1 (Fig. 13)

Basal sediment unit 1 provides evidence for an open herbaceous landscape with a limited herbaceous vegetation cover and corresponds to GS-2a. Because OM suitable for radiocarbon dating is virtually absent, it is difficult to evaluate the duration of the period represented by sediment unit 1. Assuming a sedimentation rate similar to that prevailing during the deposition of sediment unit 3 (GS-1) which is also composed of clayey silts, level 500 cm may date to before 17,200 cal yr BP, though this is an approximative assessment only, because units 1 and 3 are comparable neither climatically, nor from a point of view of vegetation cover.

All the evidence points to a cool climate resulting in low pollen concentration and the absence of biogenic carbonate sedimentation. Wind-facetted quartz, clay mineral inputs and long-distance transported *Pinus* pollen grains point to strong winds. In the lake, the accumulation of allochthonous deposits dominates, as indicated by the mineralogy and high MS values. The chironomid assemblages indicate oligo-mesotrophic conditions and well-oxygenated water in the lake basin. Sediments from this period have a weak TOM due to a weak development of soils and vegetation in the catchment area. The quasi-constant values of quartz, calcite and the <63 µm grain-size fraction suggest a relatively stable landscape over the entire period.

However, there are some indications of changes in environmental conditions. At 482–480 cm depth, the MS values undergo a first abrupt fall, coinciding with a slight rise in *Helianthemum* percentages and, more generally, herbaceous pollen concentrations (PAZ-1b/1a transition). At level 485–480 cm, LOC also marks a first quite small increase in lake productivity followed by a second at level 465 cm when an important change in chironomid fauna suggests a higher organic accumulation as well as a slight reduction of oxygen concentration. Furthermore, the clear reduction of Rcm values at 475 cm depth suggests a decrease in the wind strength and/or in the production of source regions, where an increase in the vegetation cover and a greater stabilisation of soils may be responsible for a decline of allochthonous inputs. The progressive retreat of *C. ambigua* and the increase in *Chironomus* fit well with the increase in LOC values (higher lake productivity).

Finally, a major last step of environmental changes occurs in the later part of sediment unit 1 from level 450 cm upwards. It is marked by a disappearance of kaolinite input, an abrupt fall in MS and <63 μm fraction, a rise in TeOC, while herbaceous pollen concentrations double and *Helianthemum* forms a peak. Taken together, this suggests slightly warmer conditions favouring a higher lake productivity and the development of the vegetation cover and soils on the catchment slopes, whereas wind strength decreases.

The quantified climatic parameters indicate generally cool and dry conditions during the entire period, with summer temperature (mean July) fluctuating around 10.5–12 °C (PFT and BA methods) (Fig. 11). These values are close to those inferred from the chironomid fauna, which, however, suggest a greater climate variability over the period (Fig. 11).

12.2.2. Transition between sediment units 1 and 2

All evidence points to a major warming at around 445 cm depth as indicated by the abrupt development of the biogenic carbonate sedimentation in correlation with the disappearance of the detritic input, and by heaviest oxygen-isotope values. In agreement with the pollen data, this suggests a rapid stabilisation of the catchment slopes by an increasing vegetation cover. First among the AP taxa, *Juniperus* shows a rapid expansion between levels 445.5 and 444.5 cm from 1% to 7% in less than 40 yr. It was followed by *Betula* which reaches ca 35% from 444.5 to 442.5 cm depth. Both TeOC and LOC mark an abrupt rise suggesting strong soil development and lake productivity. The aquatic fauna reveals an abrupt change with the rapid decline of *C. ambigua* between levels 446.5 and 444.5 cm.

The quantitative reconstructions from pollen data point to a summer temperature (mean July) peaking at 17–18 °C as early as level 444.5 cm. This is confirmed by the chironomid-based reconstruction, which provides a slightly delayed and lower maximum of July air temperature (15.3 °C at level 442 cm). The warming is associated with an important increase in annual precipitation (PANN) as well as in the available moisture which is also of crucial importance for vegetation development.

12.2.3. Sediment unit 2

Regarding the history of the vegetation, the sediment unit 2 record suggests a picture typical for the Lateglacial reforestation phase in the region, with a succession of juniper scrub, birch woodland and, finally, pine forest reaching a first maximum at level 400.5 cm (i.e. ca 13,600 cal yr BP). During this period, the development of the vegetation cover progressively reduces erosional processes on the catchment slopes as inferred from the decline in MS values, which stabilise from level 400 cm upwards. This fits well with the general increase in TOM (relative to LOM) reflecting the increasing development and maturation of catchment soils between 445 and 400 cm depth.

However, superimposed on this general trend, there is evidence for the occurrence of distinct cooling events responsible for regressive phases in the vegetation development. Three successive episodes of decrease in *Betula* described in Section 4 from both percentages and pollen concentrations appear to have been registered by other biotic and abiotic markers as well (Fig. 14). The first decrease of *Betula* at level 440 cm is synchronous with a climate cooling as reflected by the oxygen-isotope profile and with a peak in MS, a rise in lake level, a decrease in TOM as well as in the *Chironomus* percentages. The second phase, at 430–428 cm depth (i.e. ca 14,350 cal yr BP), appears to be less pronounced in terms of decline in

the percentages and pollen concentrations of *Betula*, but it is in phase with a rise in *Artemisia* and *Juniperus* percentages and concentrations, a negative isotope anomaly, and a higher lake level. The third phase consists of two successive birch minima at level 418–416 and 410–408 cm (ca 14,050 and 13,850 cal yr BP). It is paralleled by a well-marked second maximum of *Juniperus* percentages, a higher lake level, two decreases in TOM ratio, a slight rise in MS values at level 418 cm and less anoxic conditions as suggested by a decrease in *Polypedilum*. However, only a weak signal appears in the oxygen-isotope profile, possibly masked by detritic inputs. Taken together, these three successive phases of *Betula* decline mark distinct cooling episodes resulting in (1) less anoxic conditions in the lake basin, and (2) a clearing of the vegetation cover correlative with an increasing detrital input to the lake.

From 400 to 326 cm depth, the landscape is characterised by relatively dense pine forests (Allerød pollen zone) as reflected by quasi-constant low MS values, while maximum value of TOM/LOM ratio suggests a good maturation of catchment soils. However, like the preceding Bølling period, this warm Allerød phase was interrupted by a series of cooling episodes. Shortly after a first maximum at level 400.5 cm, both the percentages and pollen concentrations of *Pinus* show two successive declines at 394.5 and 386.5 cm depth (i.e. ca 13,550 and 13,450 cal yr BP). They are associated with two minor peaks of juniper percentages. The isotope profile indicates a cooling phase concomitant with a rise in lake level, a fall in TOC and TOM, while the chironomid fauna suggests a better-oxygenated water in the lake (see Section 5).

The next cooling episode appears less pronounced in the percentages or pollen concentrations of *Pinus* at level 363 and 355 cm (i.e. ca 12,270–12,960 cal yr BP) than by negative isotope anomalies, higher lake level as well as, between 360 and 350 cm depth, less anoxic conditions in the lake basin as inferred from the chironomid assemblages. It was followed by another short cold spell, which began before the LST deposition and was responsible for lower percentages and pollen concentration of *Pinus* at levels 346.5 and 342.5 cm, lower oxygen-isotope values at 346 and 342 cm depth, and a brief increase in the detrital input to the lake basin marked by a peak of quartz at level 345 cm.

The chironomid-based temperature record suggests two short-term decreases in summer temperature centred on ca 360 and 343 cm depth (Fig. 11). The first of these is coeval with a decrease in the Lac Lautrey ^{18}O record (Fig. 9) and may be related to the beginning of GI-1b (see Fig. 14). However, the second begins just before and ends just after the deposition of the LST, during a period which is generally considered to have featured a comparatively warm climate. Possibly this is an artefact in the record due to the application of a chironomid-temperature transfer function calibrated on mid-lake samples to a littoral sediment core.

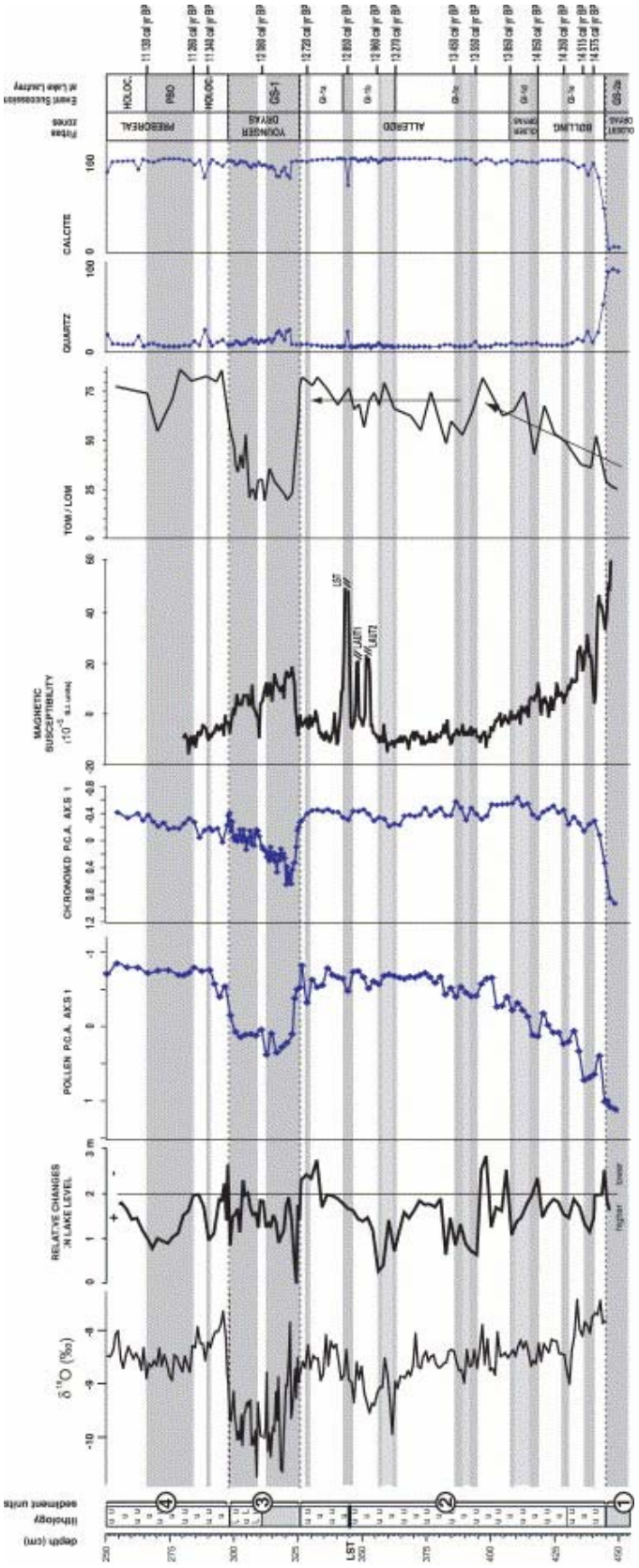

Fig. 14. Environmental synthesis for Greenland Interstadial 1, Greenland Stadial 1 and early Holocene as documented by Lautrey core 6. The pollen and chironomid data are presented using curves of scores of PCA axis 1. Grey bands correspond to cooling events documented by several biotic and/or non-biotic indicators. The right-hand column presents the event succession established from Lautrey core 6 for GI-1, GS-1 and early Holocene periods. The ages are inferred from the time-depth model presented in Fig. 12.

The last part of sediment unit 2 provides contrasting evidence for the history of environmental conditions. Maximal TOM values between 336.5 and 326.5 cm depth, as well as more anoxic conditions and a large development of the aquatic vegetation in the lake basin as inferred from the chironomid assemblages, suggest still rather favourable conditions. However, more severe climate conditions can be inferred from a general decrease in the pollen concentrations from level 330 cm concomitant with higher MS values. Moreover, a short-lived but well-marked cooling event can be observed at level 328.5 cm (i.e. ca 12,720 cal yr BP) from a conspicuous pollen concentration minimum, a fall in TOM values and a reduction of *Polypedilum* and *Glyptotendipes*, i.e. both chironomid taxa associated with more anoxic conditions and well-developed aquatic vegetation. Thus, the general trend initiated from 330 cm depth and the cool spell observed at 328.5 cm depth may be considered to be precursory signs of the next significant cooling event registered by sediment unit 3.

12.2.4. Sediment unit 3

All proxies, with the exception of the oxygen-isotope record which appears to be partly confused by detrital inputs, point to a marked cooling over the transition from sediment units 2 to 3. With respect to the lithology, the abrupt transition at level 326 cm from yellow-beige carbonate lake-marl to grey clayey silts provides a first indication of strong changes in climatic and environmental conditions. From levels 326 to 324 cm, i.e. within approximately 100 yr between 12,700 and 12,600 cal yr BP, a sudden increase in lithoclasts (Fig. 10) indicates a strong reactivation of surficial runoff. As early as level 325.75 cm, the AP percentages and concentrations show a first rapid decline followed, after a short-lived stop at 324.75 cm depth, by a second and more durable reduction from level 323.75 cm upwards. The rapid increase in MS values between 325 and 322.5 cm depth reflects increasing detrital inputs (reduction of the vegetation cover). The re-appearance of quartz at sample 322 cm and dolomite at sample 317 cm illustrates the reactivation of detrital input due to runoff and stronger wind.

In the lake basin, the chironomid fauna reacts at 325.75 cm depth and, in particular, shows a rapid re-expansion of *C. ambigua*, which had completely disappeared during GI-1. However, in contrast to the cool period documented by sediment unit 1, the calcite curve does not register a lowering at the GS-1 onset. This means that the summer temperature still allows the formation of biogenic carbonate, even if cooler temperature led to a strong reduction of the processes and consecutively of the sedimentation rate.

The chironomid-based quantitative reconstruction of climatic parameters reveals a decrease of the summer temperature from 18.4 to 15.5 °C as early as 325.5 cm depth. This is prior to the signal reconstructed from the pollen data, which indicate a cooling from 17 to 13.2–12.8 °C. In the same period, PANN and the available moisture dramatically fall. This could have led to death of local trees, lower vegetation cover and apparent increase in *Artemisia* percentage but not influx.

GS-1 as documented by sediment unit 3 shows a general trend towards a slight warming. Evidence of this general evolution can be observed in the isotopic curve, as well as in the progressive reduction of *C. ambigua*. Similarly, lake-level fluctuations, LOM percentage and MS values show a general downward trend. On the catchment slopes, the vegetation cover slightly restored as suggested by the increase in pollen concentrations from level 304.75 cm

(i.e. 11,750 cal yr BP), and the progressive disappearance of detrital yield associated with wind input and erosional processes over the catchment area.

In the middle of GS-1, at 312–310 cm depth, there is ample evidence for a short-lived warming episode which is reflected by a lowering of the MS values, a fall in lake level, peaking values of TeOC and LOC, and a decrease in *C. ambigua* concomitant with a positive oxygen-isotope anomaly. The vegetation cover gives a similar signal with the start of a slight increase in the pollen concentrations at level 310.75–308.75 cm. The PFT reconstruction also indicates a greater moisture availability during this warmer episode.

12.2.5. Sediment unit 4

At the transition from the sediment units 3 to 4, the oxygen-isotope profile gives a clear signal of an abrupt climatic warming between levels 298 and 296 cm. This favoured biogenic carbonate precipitation and resulted in a fourfold rise in sedimentation rate. The AP percentages abruptly rise at level 294.5 cm. Similarly, in the lake basin, *Chironomus* shows a continuous re-expansion from 297.75 cm depth, while *C. ambigua* is reduced to very low values at level 299.75 cm before disappearing at level 297.25 cm. On the catchment slopes, a rapid restoration of soils accompanies the development of the vegetation cover. The pollen-based quantitative reconstructions of climatic parameters suggest that the climate warming was associated with a reactivation of the hydrological cycle as shown by an increase in PANN and available moisture, while the lake-level record displays a rapid fall. The temperature maximum reconstructed from pollen data appears to be delayed in comparison with the rapidity illustrated by the various proxy data presented above. This may reflect migrational lags as shown at Gerzensee in Switzerland by Lotter et al. (2000). Moreover, the chironomid-based reconstructions indicate a warming of rather limited magnitude.

During the early Holocene, the oxygen-isotope profile gives evidence for two successive cooling events, a short one centred at level 290 cm (i.e. ca 11,340 cal yr BP) followed by a more durable negative oscillation culminating at 284–266 cm depth (i.e. ca 11,280–11,130 cal yr BP). These episodes are associated with a higher lake level as well as a more or less marked decline of *Chironomus* and a reduction of the TOM. No clear signal can be observed from the vegetation cover during either event. The chironomid-based reconstructions suggest two successive declines of the summer temperature from 18.5 to 15.5 °C and from 17.5 to 14 °C, whereas the pollen-based quantifications reveal a summer temperature decrease from 16.2 to 15.2 °C for the second episode.

13. Discussion and conclusions

13.1. A high-resolution record of climatic changes

The Lautrey data set allows the construction of a detailed sequence of climatic and environmental changes in the central Jura mountains during the Last Glacial–Interglacial transition. As discussed in Section 9, the Lautrey isotope record established from bulk sediment shows perturbations of the climatic signal probably due to detrital input from the catchment area, in particular during events GS-2a and GI-1d, and at the beginning of GS-1. However, keeping in mind these limitations and using the information provided by other proxies, the Lautrey oxygen-isotope profile can broadly be compared with that from the GRIP ice core considered as a climatic type profile (Fig. 12A). The environmental synthesis

presented in Section 12.2 reveals that, at the Lautrey site, the major forcing factor of environmental change was variation in climate such as registered by the isotope record or lake-level fluctuations. Fig. 13 and Fig. 14 summarise the succession of climatic events recognised from core 6. This sequence of events in general shows a good agreement with that established for the North Atlantic region and west-central Europe (Lotter et al., 1992; Björck et al., 1997 and Björck et al., 1998; Grafenstein et al., 1999; Ammann et al., 2000; Brauer et al., 2000) and provides some additional indications discussed below.

During GS-2a, the Lautrey record provides insights into limited environmental changes from level 482 cm upwards, clearly strengthened above 450 cm depth, i.e. at, respectively, ca 16,500 and 15,000 cal yr BP (ages extrapolated from the sedimentation rate). The first change may find an equivalent in the start of a shrub-phase with *Betula nana*, *Salix* and *Juniperus* (i.e. Swiss pollen zone CHb-1c, Ammann et al., 1996) dated to 13,600±200 ^{14}C yr BP (i.e. 16,672–15,997 cal yr BP) at Rotsee, 13,360±280 ^{14}C yr BP (i.e. 16,448–15,662 cal yr BP) at Lobsigensee, and to 13,335±120 ^{14}C yr BP (i.e. 16,276–15,755 cal yr BP) at Schleinsee (Ammann and Lotter, 1989). The second change at level 450 cm may be coeval with the substantial expansion of *Juniperus* before the radiocarbon plateau at 12,700–12,600 ^{14}C yr BP and observed in the upper part of the Swiss pollen zone CHb-1c at ca 13,000 ^{14}C yr BP (i.e. 15,800–15,300 cal yr BP) and in the French northern Alps at 13,040 ^{14}C yr BP (David, 2001). These data recall the discussion by Walker et al. (2003) about a possible rise in temperature in western Europe earlier than the 14,700 cal yr BP Greenland thermal maximum.

During GI-1, the Lautrey data set gives insights into the occurrence of two cooling events between the thermal maximum at 14,700 cal yr BP and the GI-1d event (Fig. 14). At Gerzensee, two cold episodes may be inferred from increases in NAP and oxygen-isotope anomalies within the pollen zones CHb-2 and 3a (Lotter et al., 1992). Such Intra-Bølling Cold Periods (IBCPs) have also been documented by various palaeoclimatic records from west-central Europe (Bégeot, 2000; Magny and Richoz, 2000; David, 2001), the Norwegian Sea (Karpuz and Jansen, 1992), the Cariaco Basin (Hughen et al., 1998) and the Greenland ice cores (Johnsen et al., 1992; Stuiver et al., 1995).

Furthermore, the section 394.5–386.5 cm (i.e. ca 13,550–13,450 cal yr BP) of the Lautrey record confirms the occurrence of an additional cold event (GS-1c2 as defined by Brauer et al. in 2000 from the Meerfelder Maar sequence in Germany). This event is well marked in both the GRIP and Ammersee isotope records, where it is dated to ca 13,450 cal yr BP (Johnsen et al., 1992; Grafenstein et al., 1999) and has also been observed in Coleopteran MCR data from Gransmoor in NE England (Walker et al., 2003) and in the pollen profile from Längsee in Austria (Schmidt et al., 2002). It may also have equivalents in an oxygen-isotope negative anomaly and/or an episode of *Pinus* decline within zone CHb-4a at Gerzensee in Switzerland (Lotter et al., 1992).

The very short-lived cooling observed in sample 328.5 cm (i.e. 12,720 cal yr BP) between the LST deposition and the GS-1 onset may find an equivalent at Soppensee, Switzerland, where core SO86-14 shows a short pronounced decline in *Pinus* dominance correlative with a marked peak of *Betula* and a slight increase in *Artemisia* between the LST and the GS-1 start (Lotter et al., 1992). More generally speaking, the last cold episode of the Gerzensee oscillation observed at 346.5–342.5 cm depth and the general cooling trend illustrated by a clear decrease in pollen concentrations from 355 cm depth (i.e. since the GI-1b event and before the GS-1 start), may be compared with the long-term decrease in temperature reconstructed as early as 13,100 cal yr BP at Llanilid in South Wales (Walker et al., 2003).

In the middle of GS-1, the conspicuous short-lived warm event recognised at 312–310 cm depth (ca 12,080 cal yr BP) is paralleled by an intriguing brief positive oxygen-isotope anomaly in both the GRIP and Ammersee records to ca 12,050 cal yr BP. The pollen record established at Lake Nimgun, south-western Alaska (Hu et al., 2002) and a sea-surface temperature record from the central Mediterranean sea (Sbaffi et al., 2004) reveal a similar short-lived warming episode dated to 12,100–12,000 cal yr BP. The general warming trend shown by most of the Lautrey data over the GS-1 is similar to that illustrated by the GRIP oxygen-isotope and Calcium records (Brauer et al., 2000), as well as by the Ammersee and Gerzensee ^{18}O records (Grafenstein et al., 1999; Ammann et al., 2000).

Finally, the two successive cooling events centred at ca 11,350 and 11,200 cal yr BP have equivalents in the GRIP record, the second corresponding to the PBO (Lotter et al., 1992; Björck et al., 1997) and the first to a precursor episode. Such multiple cold oscillations during the early Holocene have also been observed on the Swiss Plateau (Magny, 2001; Magny et al., 2003) and in Sweden (Björck and Wastergard, 1999). The possible correlations addressed above between brief cooling events observed at Lake Lautrey and other west European sites in addition to the more classic GI-1d, GI-1b and PBO oscillations, suggest interesting working hypotheses, but still need to be tested by further investigations in other sites on the basis of high-resolution analysis and chronology.

13.2. Comparison of the quantitative reconstructions

Regarding the quantitative reconstructions of climatic parameters, Table 4 presents a comparison of results obtained from the various methods used at Lautrey as well as (1) from pollen and cladocera-based transfer functions at Gerzensee in Switzerland (Lotter et al., 2000), (2) from coleopteran data in the Swiss Plateau (Gaillard and Lemdahl, 1994; Coope and Elias, 2000) and in the Paris Basin (Limondin-Lozouet et al., 2002), and (3) from geological–palaeoecological data and AGCM experiments in Europe (Isarin and Bohncke, 1999; Renssen and Isarin, 2001; Renssen and Bogaart, 2003). Additional data are provided by previous studies at Lake Le Locle in the Swiss Jura mountains (Magny et al., 2001). The following discussion focuses mainly on the major periods of climatic changes.

Table 4. : Comparison of quantitative palaeoclimate reconstructions in west-central Europe using various approaches

Sites of regions	**References**	**Method**	**GS-2**	**GI-1e**	**GI-lb**	**GI-1/GS-1 transition**	**GS-1 latter part**	**GS-1/Proboreal transition**	**Proboreal oscillation**
Lake Lautrey 788 m a.s.l.	This study	Chironomids	11–12 °C	15.5 °C (≈+4 °C)	16.8–15 °C (≈−2 °C)	18.4–15.5 °C (≈−3 °C)	13.5–14 °C (≈+0.5 °C)	13.9–15.5 °C (≈+1.5 °C)	17.5–14 °C (≈−3.5 °C
		Pollen data (PFT)	11–12 °C	16.5 °C (≈+4.5X)	?	17–13,2 °C (≈−4 °C)		Lag, 13–l6 °C (≈+3 °C)	16.2–l5.2 °C (≈−1 °C
		Pollen data (BAM)	11.5–12 °C	16.5 °C (≈+5.5 °C)	?	17–12.8 °C (≈−4 °C)	7		
		Pollen data (PFT)	10.5–ll.5 °C	500 mm	7	400 mm	450 mm	500 mm	470 mm
		Relative lake level	300 mm	Lower	Higher	Higher	Lower	Lower	Higher
Lake Le Lock, 915 m a.s.l.	Magny et al. (2001)	Pollen and lake-level data					13.2–l4.2 °C (≈+l °C)	14–16 °C (≈+2 °C)	16–l4 °C (≈−2 °C)
Gerzensee, 603 m a.s.l.	Ammann et al. (2000) and Letter etal. (2000)	Pollen data (CF)			12–10.7 °C (≈−1.3 °C)	11.5–8.7 °C (≈−3 °C)	9–10 °C (≈+l °C)	10–12 °C (≈+2 °C)	12–ll.5 °C (≈−0.5 °C)
		Cladocera (CF)			12–ll.2 °C (≈−0.8 °C)			9–ll.5 °C (≈+2.5 °C)	
Hauterive-Champreveyres, 428 m a.s.l. (Lake Neuchatel)	Coope and Elias (2000)	Coleoptera (MCR)	July: 9 °C; January: −25 °C	July: 16 °C; January: 0 °C					
Grand-Marais, 587 m a.s.l.	Gaillard and Lemdahl (1994)	Coleoptera (MCR)	July: 10 °C; January:−10 °C	July: 15 °C; January: 0 °C					
South-Western Switzerland	Wohlfarth et al. (1994)	Pollen and isotope data		12–14 °C		≈−3 to −4 °C			
West-central Europe	Isarin and Bohncke (1999), Renssen and Isarin (2001) and Renssen and Bogaart (2003)	Geological-ecological data, and AGCM		≈10 °C	12 °C (≈+3 °C)			10–11 to 10–12 °C (≈+1 °C)	9–11–12–14 °C (≈+3 °C)

Sites of regions	References	Method	GS-2	GI-1e	GI-lb	GI-1/GS-1 transition	GS-1 latter part	GS-1/Preboreal transition	Preboreal oscillation
Paris Basin	Limondin-Lozouet et al. (2002)	Coleoptera (MCR)		Conty: 15–19 °C; Houdancourt 17–18 °C					
		River channels	Braided	Incision (>meandering)		Braided, accumulation		Incision (>meandering)	

Note: The location of the sites is indicated in Fig. 1. The data for west-central Europe were originally published as estimations at sea-level elevation and they have been corrected for this study referring to the altitude of Lake Lautrey and assuming a lapse rate of 0.6 °C per 100 m.

Although general agreement can be observed between the data to outline an identical succession of warming (GS-2a/GI-1e and GS-1/Preboreal transitions) and cooling (GS-2a and GS-1) phases between the various sites, there are also discrepancies depending on the periods and/or methods used. Generally speaking, the temperature levels reconstructed from the Lautrey and Le Locle data sets for cool and warm periods are closely similar to those inferred from coleopteran data, but higher than those reconstructed at Gerzensee or in west-central Europe using other approaches. The temperature values obtained at Lautrey and Le Locle for the beginning of the GI-1 and the Holocene are also closer to those prevailing today in the study area than the reconstructed temperature obtained from other sites. Furthermore, the relatively high summer temperature reconstructed for GS-1 at Lautrey in comparison with those obtained for GS-2a fits well with the continuity of the authigenic carbonate sedimentation during the Younger Dryas cold event at Lautrey and Le Locle.

Moreover, the magnitude of the temperature changes reconstructed at Lautrey, Le Locle, Gerzensee and more generally in west-central Europe, most often differs by a factor 2. For example, the magnitude of the reconstructed cooling during the PBO ranges from 0.5 to 3.5 °C. These divergences are related to differences in the techniques of reconstruction (BA and PFT methods, transfer functions) and in modern databases used, as well as in the sensitivity of the climatic indicators used (chironomids, cladocera, pollen, geological features). Furthermore, non-climatic factors may also have an impact on the biotic indicators used for climatic reconstructions (Ammann et al., 2000).

Regarding the annual precipitation and its seasonal distribution throughout the Last Glacial–Interglacial transition at Lautrey, the pollen-based reconstructions clearly show a reactivation of the hydrological cycle at the onset of GI-1 and Holocene marked by an increase in PANN and available moisture. This is paralleled by an abrupt increase in snow accumulation over the Greenland ice-sheet during the same period (Alley et al., 1993). Such a general reactivation of the hydrological cycle probably reflects the retreat of sea ice (Renssen and Isarin, 2001) and increased evaporation over the ocean due to higher temperatures. The phases of rapid warming at 14,700 and 11,500 cal yr BP were also characterised by a major lake-level lowering in the Jura mountains and on the Swiss Plateau (Magny, 2001) and an important incision of valley floors in western Europe (Antoine, 1997; Vandenberghe, 2003). Keeping in mind that the carbonate concretions used to reconstruct lake levels (see Section 10) form during the warm season, an increase in PANN suggests a seasonality marked by dry summers and wet winters for the beginning of GI-1e and Preboreal. This implies that the lake-level lowering is related to summer dryness, while river incision may be a result of increasing

precipitation and higher discharge during the winter, or the snow melting season in addition to a possible impact of changes in vegetation cover (Vandenberghe, 2003). Conversely, the rise in lake level and the return of rivers to braided channels at the beginning of GS-1 suggest an opposite pattern of seasonality marked by wetter summers and drier winters as a result of a southward shift of (1) the sea ice during the winter and (2) the storm track in the summer in agreement with AGCM experiments (Renssen and Isarin, 2001; Renssen and Bogaart, 2003).

13.3. The response of terrestrial and aquatic organisms to climatic changes

The various biotic and abiotic records presented in this paper provide a coherent picture of local environmental and climatic changes around Lake Lautrey during the Last Glacial–Interglacial transition. They give insights into the dynamics of the ecosystem and the response of terrestrial and aquatic organisms to climatic changes. The warmer periods such as GI-1 and the Preboreal are characterised by an increasing biodiversity and complexity of the ecosystems, which show a great sensitivity to multiple successive climatic oscillations. However, the relative stability of the MS signal (except for the peaks due to tephras) and TOM values above 400 cm depth (except for secondary oscillations) indicates that, after the completion of the reforestation, the vegetation cover is less sensitive to climate impact than during the first part of the Lateglacial Interstadial. Finally, the MS and TOM curves, and the pollen diagram indicate that the restoration of the forest after GS-1 was much more rapid than after GS-2a.

Furthermore, biotic and abiotic indicators may not show proportionate signals in response to an identical forcing factor. An illustration of this is given at 483–480 cm depth by the contrast between the slight increase in herbaceous pollen concentration and the considerably more abrupt fall in MS values. This probably reflects non-linear processes associated with critical thresholds, the crossing of which governs the geomorphological (or biological) response to climatic changes (Walker et al., 2003). Conversely at the GS-1 onset, because the signals given by MS, quartz and dolomite mainly depend on the reduction in forest density, these indicators appear to be late in comparison with the chironomids and the arboreal pollen concentration.

A focus on the diverse records around the three major phases of climate change at the GS-2a/GI-1e, GI-1a/GS-1 and GS-1/Preboreal transitions reveals that indicators show responses that are more or less simultaneous (Fig. 14). The most striking evidence for this can be observed at the beginning of the GI-1 and at the GS-1 start. At level 444.5 cm, i.e. less than ca 20 yr after the abrupt change from allochthonous to authigenic sedimentation at level 445 cm, aquatic and terrestrial organisms mark a first clear expansion with the rapid development of *Juniperus* (level 444.5 cm) and *Betula* (level 442.5 cm) on the catchment area, while (1) *Chironomus* marks an expansion as early as level 444.5 cm and a first peak at 442.5 cm depth (i.e. ca 65 yr after the onset of biogenic calcite deposition), and (2) *C. ambigua* strongly declines at level 444.5 cm and has almost disappeared at level 442.5 cm. The LOC and TeOC curves indicate a synchronous signal at level 444.5 cm.

At the beginning of GS-1, the first responses of the vegetation and chironomid fauna occur simultaneously at 325.75 cm depth. *C. ambigua* appears at level 324.75 cm and reaches maximal values as early as 322.75 cm. Thus, within ca 150 yr, the chironomid assemblages show a very different picture. The rapidity of the change is nearly similar for the vegetation cover.

At the beginning of the Holocene, the chironomid taxa react at 297.75 cm depth (re-appearance and continuous re-expansion of *Chironomus*), while *C. ambigua* has completely disappeared at level 297.25 cm (i.e. ca 30 yr after level 298 cm). The pollen percentages indicate a first restoration of the forest at 296.5 cm depth, i.e. ca 70 yr after the shift to warm chironomid assemblages. Pollen concentrations show a rapid increase at 294.5 cm depth. Thus, as observed by Ammann et al. (2000) at Gerzensee, the response of organisms appears less telescoped during less abrupt climatic changes like the GS-1/Preboreal transition. In that case, as suggested by Birks et al. (2000) from Lake Krakenes in Norway and by Yu (2000) from Twiss Marl Pond in Canada, the earliness of the chironomid response observed at Lautrey supports the view that, in addition to terrestrial beetles (Coope et al., 1998), aquatic organisms are probably the best recorders of Lateglacial climatic changes.

Acknowledgments

Financial support for this study was provided by the French CNRS (program ECLIPSE). Isotope measurements were carried out during a CLIVARNET project financed by the Dutch Science Foundation NWO. The authors express their sincere thanks to J.C Rougeot for his help with the figure drawings, and to John Olsen for his help with the English language. An earlier draft of this manuscript benefited greatly from comments by H.H. Birks and A.F. Lotter. Finally, we acknowledge J.J. Lowe and an anonymous reviewer for their helpful and constructive remarks to improve the manuscript.

References

Aalbersberg et al., 1999 G. Aalbersberg, C.J. Beets, J.F. Vandenberghe and A.F. Coevert, Natural climate variability in the Lateglacial: high resolution stable isotope analyses and geochemistry from Jura lakes (Eastern France), *Terra Nostra* **10** (1999), pp. 15–18.

Alley et al., 1993 R.B. Alley, D.A. Meese, C.A. Shuman, A.J. Gow, K.C. Taylor, P.M. Grootes, J.W.C. White, M. Ram, E.D. Waddington, P.A. Mayewski and G.A. Zielinski, Abrupt increase in Greenland snow accumulation at the end of the Younger Dryas event, *Nature* **362** (1993), pp. 527–529.

Ammann and Lotter, 1989 B. Ammann and A. Lotter, Late-Glacial radiocarbon and palynostratigraphy on the Swiss Plateau, *Boreas* **18** (1989), pp. 109–126.

Ammann et al., 1996 B. Ammann, M.-J. Gaillard and A.F. Lotter, Switzerland. In: B.E. Berglund, H.J.B. Birks, M. Ralska-Jasiewiczowa and H.E. Wright, Editors, *Palaeoecological Events During the Last 15000 Years*, Wiley, New York (1996), pp. 155–170.

Ammann et al., 2000 B. Ammann, H.J.B. Birks, S.J. Brooks, U. Eicher, U. von Grafenstein, W. Hofman, G. Lemdahl, J. Schwander, K. Tobolski and L. Wick, Quantification of biotic responses to rapid climatic changes around the Younger Dryas—a synthesis, *Palaeogeography, Palaeoecology, Palaeoclimatology* **159** (2000), pp. 313–349.

Amorosi et al., 2002 A. Amorosi, M.C. Centineo, E. Dinelli, F. Luchini and F. Tateo, Geochemical and mineralogical variations as indicators of provenance changes in Late Quaternary deposits of SE Po Plain, *Sedimentary Geology* **151** (2002), pp. 273–292.

Antoine, 1997 P. Antoine, Modifications des systèmes fluviatiles à la transition Pléniglaciaire–Tardiglaciaire et à l'Holocène: l'exemple du bassin de la Somme (Nord de la France), *Géographie Physique et Quaternaire* **51** (1997), pp. 93–106.

de Beaulieu et al., 1994 J.-L. de Beaulieu, H. Richard, P. Ruffaldi and J. Clerc, History of vegetation, climate and human action in the French Alps and the Jura over the last 15 000 years, *Dissertationes Botanicae* **234** (1994), pp. 253–276.

Bgeot, 2000 Bégeot, C., 2000. Histoire de la végétation et du climat au cours du Tardiglaciaire et du début de l'Holocène sur le Massif jurassien central à partir de l'analyse pollinique et des macrorestes végétaux. Ph.D., University of Franche Comté, Besançon.

Bertrand, 1992 P. Bertrand, S. Brocero, E. Lallier-Vergès, N. Tribovillard and E. Bonifay, Sédimentation organique lacustre et paléoclimats du Pleistocène aux moyennes latitudes: exemple du lac du Bouchet, Haute Loire, France, *Bulletin de la Société Géologique de France* **163** (1992), pp. 427–433.

Birks and Wright, 2000 H.H. Birks and H.E. Wright, Introduction to the reconstruction of the late-glacial and early Holocene aquatic ecosystems at Krakenes Lake, Norway, *Journal of Paleolimnology* **23** (2000), pp. 1–5.

Birks et al., 2000 H.H. Birks, R.W. Battarbee and H.J.B. Birks, The development of the aquatic ecosystem at Krakenes Lake, western Norway, during the late-glacial and early Holocene—a synthesis, *Journal of Paleolimnology* **23** (2000), pp. 91–114.

Björck and Wastergard, 1999 J. Björck and S. Wastergard, Climate oscillations and tephrochronology in eastern middle Sweden during the last glacial–interglacial transition, *Journal of Quaternary Science* **14** (1999), pp. 399–410.

Björck et al., 1996 S. Björck, B. Kromer, S. Johnsen, O. Bennike, D. Hammarlund, G. Lemdahl, G. Possnert, T.L. Rasmussen, B. Wohlfarth, C.U. Hammer and M. Spurk, Synchronized terrestrial-atmospheric deglacial records around the North-Atlantic, *Science* **274** (1996), pp. 1155–1160

Björck et al., 1997 S. Björck, M. Rundgren, O. Ingolfsson and S. Funder, The Preboreal oscillation around the Nordic seas: terrestrial and lacustrine responses, *Journal of Quaternary Science* **12** (1997), pp. 455–465.

Björck et al., 1998 S. Björck, M.J.C. Walker, L.C. Cwynar, S. Johnsen, K.-L. Knudsen, J.L. Lowe, B. Wohlfarth and INTIMATE Members, An event stratigraphy for the last termination in the North Atlantic region based on the Greenland ice-core record: a proposal by the INTIMATE group, *Journal of Quaternary Science* **13** (1998), pp. 283–292.

van der Bogaard and Schmincke, 1985 P. van der Bogaard and H.U. Schmincke, Laacher See Tephra: a widespread isochronous late Quaternary tephra layer in central and northern Europe, *Geological Society of America Bulletin* **96** (1985), pp. 1554–1571.

Bohncke and Vandenberghe, 1991 S.J.P. Bohncke and J. Vandenberghe, Palaeohydrological developments in the Southern Netherlands during the last 15 000 years. In: L. Starkel, K.J.

Gregory and J.B. Thornes, Editors, *Temperate Palaeohydrology*, Wiley, Chichester and New York (1991), pp. 253–281.

Bossuet et al., 1997 G. Bossuet, H. Richard, M. Magny and M. Rossy, Nouvelle occurrence du Laacher See Tephra dans le Jura central. L'étang du Lautrey (France), *Comptes Rendus Académie des Sciences, Paris* **325** (1997), pp. 43–48.

Bossuet et al., 2000 G. Bossuet, C. Camerlinck, M. Dabas and J. Martin, Contribution des méthodes géophysiques (électrique, électromagnétique et radar sol) à l'étude des dépressions lacustres. L'exemple du Lautrey (Jura, France), *Ecolgae Geologicae Helvetiae* **93** (2000), pp. 147–156.

Bourdon et al., 2000 S. Bourdon, F. Laggoun-Defarge, O. Maman, J.R. Disnar, B. Guillet, S. Derenne and C. Largeau, Organic matter sources and early diagenetic degradation in a tropical peaty marsh (Tritivakely, Madagascar). Implications for environmental reconstrcution during the Sub-Atlantic, *Organic Geochemistry* **31** (2000), pp. 421–438.

Brauer et al., 1999 A. Brauer, C. Endres, C. Günter, T. Litt, M. Stebich and J.F.W. Negendank, High resolution sediment and vegetation responses to Younger Dryas climate change in varved lake sediments from Meerfelder Maar, Germany, *Quaternary Science Reviews* **18** (1999), pp. 321–329.

Brauer et al., 2000 A. Brauer, C. Günter, S.J. Johnsen and J.F.W. Negendank, Land-ice teleconnections of cold climatic periods during the last Glacial/Interglacial transition, *Climate Dynamics* **16** (2000), pp. 229–239.

Brodersen and Lindegaard, 1999 K.P. Brodersen and C. Lindegaard, Mass occurrence and sporadic distribution of *Corynocera ambigua* Zetterstedt (Diptera, Chironomidae) in Danish lakes. Neo- and palaeolimnological records, *Journal of Paleolimnology* **22** (1999), pp. 41–52.

Brooks and Birks, 2000 S. Brooks and H.J.B. Birks, Chironomid-inferred late-glacial and early Holocene mean July air temperatures for Kråkenes Lake, western Norway, *Journal of Paleolimnolgy* **23** (2000), pp. 77–89.

Clark et al., 2001 P.U. Clark, S.J. Marshall, G.K.C. Clarke, S.W. Hostetler, J.M. Licciardi and J.T. Teller, Freshwater forcing of abrupt climate change during the last glaciation, *Science* **293** (2001), pp. 283–287.

Coope and Elias, 2000 G.R. Coope and S.A. Elias, The environment of Upper Palaeolithic (Magdalenian and Azilian) hunters at Hauterive-Champréveyres, Neuchâtel, Switzerland, interpreted from coleopteran remains, *Journal of Quaternary Science* **15** (2000), pp. 157–175.

Coope et al., 1998 G.R. Coope, G. Lemdahl and J.J. Lowe, Temperature gradients in northern Europe during the last glacial–interglacial transition (14–9 ^{14}C kyr BP) interpreted from coleopteran assemblages, *Journal of Quaternary Science* **13** (1998), pp. 419–433.

Cour, 1974 P. Cour, Nouvelles techniques de détection des flux et des retombées polliniques: étude de la sédimentation des pollens et des spores à la surface du sol, *Pollen et Spores* **1** (1974), pp. 103–141.

David, 2001 F. David, Le tardiglaciaire des Etelles, *Comptes Rendus Académie des Sciences, Paris* **324** (2001), pp. 373–380.

Disnar et al., 2003 J.R. Disnar, B. Guillet, D. Keravis, C. Di-Giovanni and D. Sebag, Soil organic matter (SOM) characterization by Rock-Eval pyrolysis: scope and limitations, *Organic Geochemistry* **34** (2003), pp. 327–343.

Eicher, 1987 U. Eicher, Die spätglazialen sowie frühpostglazialen Klimaverhältnisse im Bereich der Alpen: Sauerstoffisotopenkurven kalkhaltiger Sedimente, *Geographica Helvetica* **2** (1987), pp. 637–642.

Espitalié et al., 1985 J. Espitalié, G. Deroo and F. Marquis, La pyrolyse Rock-Eval et ses applications, *Revue Institut Français du Pétrole* **40** (1985), p. 6 563–579 and 755–784.

Friedrich et al., 1999 M. Friedrich, B. Kromer, M. Spurk, J. Hofman and K.F. Kaiser, Paleo-environment and radiocarbon calibration as derived from Lateglacial/Early Holocene tree-ring chronologies, *Quaternary International* **61** (1999), pp. 27–39.

Gaillard and Lemdahl, 1994 M.J. Gaillard and G. Lemdahl, Lateglacial insect assemblages from Grand-Marais, south-western Switzerland—climatic implications and comparison with pollen and plant macrofossil data, *Dissertationes Botanicae* **234** (1994), pp. 287–308.

Gaillard and Moulin, 1989 M.J. Gaillard and B. Moulin, New results on the Late-glacial history and environment of the lake of Neuchâtel (Switzerland). Sedimentological and palynological investigations at the Paleolithic site of Hauterive-Champréveyres, *Ecolgae Geologicae Helvetiae* **82** (1989), pp. 203–218.

Grafenstein et al., 1999 U. Grafenstein, H. Erlenkeuser, A. Brauer, J. Jouzel and S.J. Johnsen, A mid-European decadal isotope-climate record from 15,500 to 5000 years BP, *Science* **284** (1999), pp. 1654–1657.

Guiot, 1990 J. Guiot, Methodology of palaeoclimatic reconstruction from pollen in France, *Palaeogeography, Palaeoclimatology, Palaeoecology* **80** (1990), pp. 49–69.

Guiot et al., 1993 J. Guiot, S.P. Harrison and I.C. Prentice, Reconstruction of Holocene precipitation patterns in Europe using pollen and lake-level data, *Quaternary Research* **40** (1993), pp. 139–149.

Harrison et al., 1993 S.P. Harrison, I.C. Prentice and J. Guiot, Climatic controls on Holocene lake-level changes in Europe, *Climate Dynamics* **8** (1993), pp. 189–200

Heiri, 2001 Heiri, O., 2001. Holocene palaeolimnology of Swiss mountain lakes reconstructed using subfossil chironomid remains. Ph.D. Thesis, Inauguraldissertation der Philosophisch-naturwissenschaftlichen Fakultät der Universität Bern.

Heiri and Lotter, 2001 O. Heiri and A.F. Lotter, Effect of low count sums on quantitative environmental reconstructions: an example using subfossil chironomids, *Journal of Paleolimnology* **26** (2001), pp. 343–350.

Heiri and Millet, 2005 O. Heiri and L. Millet, Reconstruction of Late Glacial summer temperatures from chironomid assemblages in Lac Lautrey (Jura, France), *Journal of Quaternary Science* **20** (2005), pp. 1–12.

Heiri et al., 2003a O. Heiri, H.J.B. Birks, S.J. Brooks, G. Velle and E. Willassen, Effects of within-lake variability of fossil assemblages on quantitative chironomid-inferred temperature reconstruction, *Palaeogeography, Palaeoclimatology, Palaeoecology* **199** (2003), pp. 95–106.

Heiri et al., 2003b O. Heiri, A.F. Lotter, S. Hausmann and F. Kienast, A chironomid-based Holocene summer air temperature reconstruction from the Swiss Alps, *The Holocene* **13** (2003), pp. 477–484.

Higgitt et al., 1991 S.R. Higgitt, F. Oldfield and P.G. Appleby, The record of land use change and soil erosion in the late Holocene sediments of the Petit Lac d'Annecy, eastern France, *The Holocene* **1** (1991), pp. 14–28.

Hoek, 2001 W.Z. Hoek, Vegetation response to the 14.7 and 11.5 ka cal. BP climate transitions: is vegetation lagging climate?, *Global and Planetary Change* **30** (2001), pp. 103–115.

Hofmann, 1971 W. Hofmann, Zur Taxonomie und Palökologie subfossiler Chironomiden (Dipt.) in Seesedimenten, *Archiv für Hydrobiologie Beiheft Ergebnisse der Limnologie* **6** (1971), pp. 1–50.

Hofmann, 1986 W. Hofmann, Chironomid analysis. In: B.E. Berglund, Editor, *Handbook on Holocene Palaeoecology and Palaeohydrology*, Wiley, Chichester (1986), pp. 715–727.

Holtzappfel, 1985 Holtzappfel, T., 1985. Les minéraux argileux. Préparation. Analyse diffractométrique et détermination. Société Géologique du Nord, 12.

Hu et al., 2002 F.S. Hu, B.Y. Lee, D.S. Kaufman, S. Yoneji, D.M. Nelson and P.D. Henne, Response of tundra ecosystem in southwestern Alaska to Younger-Dryas climatic oscillation, *Global Change Biology* **8** (2002), pp. 1156–1163.

Hughen et al., 1998 K.A. Hughen, J.T. Overpeck, S.J. Lehman, M. Kashgarian, J. Southon, L.C. Peterson, R. Alley and D.M. Sigman, Deglacial changes in ocean circulation from an extended radiocarbon calibration, *Nature* **391** (1998), pp. 65–68.

Isarin and Bohncke, 1999 R.F.B. Isarin and S.J.P. Bohncke, Mean July temperatures during the Younger Dryas in northwestern and central Europe as inferred from climate indicator plant species, *Quaternary Research* **51** (1999), pp. 158–173.

Johnsen et al., 1992 S.J. Johnsen, H.B. Clausen, W. Dansgaard, K. Fuhrer, N. Gundestrup, C.U. Hammer, P. Iversen, J. Jouzel, B. Stauffer and J.P. Steffensen, Irregular glacial interstadials recorded in a new Greenland ice core, *Nature* **359** (1992), pp. 311–313.

Juvigné et al., 1996 E. Juvigné, B. Bastin, G. Delibrias, J. Evin, M. Gewelt, E. Gilot and M. Streel, A comprehensive pollen- and tephra-based chronostratigraphic model for the Late Glacial and Holocene periods in the French Massif Central, *Quaternary International* **34-36** (1996), pp. 113–120.

Karpuz and Jansen, 1992 N.K. Karpuz and E. Jansen, A high-resolution diatom record of the last deglaciation from the SE Norwegian Sea: documentation of rapid climatic changes, *Paleoceanography* **7** (1992), pp. 499–520.

Kubler, 1987 Kubler, B., 1987. Dosage quantitative des minéraux des roches sédimentaires par diffraction X. Cahiers de l'Institut de Géologie de Neuchâtel, série ADX.

Larocque, 2001 I. Larocque, How many chironomid head capsules is enough? A statistical approach to determine sample size for paleoclimatic reconstruction, *Palaeogeography, Palaeoclimatology, Palaeoecology* **172** (2001), pp. 133–142.

Limondin-Lozouet et al., 2002 N. Limondin-Lozouet, A. Bridault, C. Leroyer, P. Ponel, P. Antoine, C. Chaussé, A.V. Munaut and J.F. Pastre, Evolution des écosystèmes de fond de vallée en France septentrionale au cours du Tardiglaciaire: l'apport des indicateurs biologiques. In: J.P. Bravard and M. Magny, Editors, *Variations paléohydrologiques en France depuis 15 000 ans*, Errance, Paris (2002), pp. 31–48.

Lotter et al., 1992 A.F. Lotter, H.J.B. Birks, U. Eicher and U. Siegenthaler, Late-glacial climatic oscillations as recorded in Swiss lake sediments, *Journal of Quaternary Science* **7** (1992), pp. 187–204.

Lotter et al., 1997 A.F. Lotter, H.J.B. Birks, W. Hofman and A. Marchetto, Modern diatom, Cladocera, chironomids and chrysophyte cyst assemblages as quantitative indicators for the reconstruction of past environmental conditions in the Alps. I. Climate, *Journal of Paleolimnology* **18** (1997), pp. 395–420.

Lotter et al., 2000 A.F. Lotter, H.J.B. Birks, U. Eicher, W. Hofman, J. Schwander and L. Wick, Younger Dryas and Allerod summer temperatures at Gerzensee (Switzerland) inferred from fossil pollen and cladoceran assemblages, *Palaeogeography, Palaeoecology, Palaeoclimatology* **159** (2000), pp. 349–362.

Lowe J., 1994 Ed. Lowe J., Climate changes in areas adjacent to the North Atlantic during the last Glacial–Interglacial transition, *Journal of Quaternary Science* **9** (1994), pp. 93–198.

Lowe et al., 1999 J.J. Lowe, H.H. Birks, S.J. Brooks, G.R. Coope, D.D. Harkness, F.E. Mayle, C. Sheldrick, C.S.M. Turney and M.J.C. Walker, The chronology of palaeoenvironmental changes during the Last Glacial–Holocene transition: towards an event stratigraphy for the British Isles, *Journal of Geological Society, London* **156** (1999), pp. 397–410.

Magny, 1992a M. Magny, Sédimentation et dynamique de comblement dans les lacs du Jura au cours des 15 derniers millénaires, *Revue d'Archéométrie* **16** (1992), pp. 27–49.

Magny, 1992b M. Magny, Holocene lake-level fluctuations in Jura and the northern subalpine ranges, France: regional pattern and climatic implications, *Boreas* **21** (1992), pp. 319–334.

Magny, 1995 M. Magny, Paleohydrological changes in Jura (France) and climatic oscillations around the North Atlantic from Allerod to Preboreal, *Geographie Physique et Quaternaire* **49** (1995), pp. 401–408.

Magny, 1998 Magny, M., 1998. Reconstruction of Holocene lake-level changes in the Jura (France): methods and results. In: Harrison, S.P., Frenzel, B., Huckried, U., Weiss, M., (Eds.), Palaeohydrology as Reflected in Lake-Level Changes as Climatic Evidence for Holocene Times. Paläoklimaforschung 25, 67–85.

Magny, 2001 M. Magny, Palaeohydrological changes as reflected by lake-level fluctuations in the Swiss Plateau, the Jura mountains and the northern French Pre-Alps during the Last Glacial–Holocene transition: a regional synthesis, *Global and Planetary Change* **30** (2001), pp. 85–101.

Magny and Richoz, 2000 M. Magny and I. Richoz, Lateglacial lake-level changes at Montilier-Strandweg, Lake Morat, Switzerland and their climatic significance, *Quaternaire* **11** (2000), pp. 129–144.

Magny et al., 2001 M. Magny, J. Guiot and P. Schoellammer, Quantitative reconstruction of Younger Dryas to mid-Holocene paleoclimates at Le Locle, Swiss Jura, using pollen and lake-level data, *Quaternary Research* **56** (2001), pp. 170–180.

Magny et al., 2003 M. Magny, N. Thew and P. Hadorn, Late-glacial and early Holocene changes in vegetation and lake-level at Hauterive/Rouges-Terres, Lake Neuchâtel (Switzerland), *Journal of Quaternary Science* **18** (2003), pp. 31–40.

Meyers and Lallier-Vergès, 1999 P. Meyers and E. Lallier-Vergès, Lacustrine sedimentary organic matter records of Late Quaternary paleoclimates, *Journal of Paleolimnology* **21** (1999), pp. 345–372.

Millet et al., 2003 L. Millet, V. Verneaux and M. Magny, Lateglacial paleoenvironmental reconstruction using subfossil chironomid assemblages from Lake Lautrey (Jura, France), *Archives für Hydrobiologie* **156** (2003), pp. 405–429.

Moore and Reynolds, 1997 D.M. Moore and R.C.J. Reynolds, X-ray Diffraction and the Identification and Analysis of Clay Minerals (second ed), Oxford University Press, New York (1997).

Nolan et al., 1999 S.R. Nolan, J. Bloemendal, J.F. Boyle, R.T. Jones, F. Oldfield and M. Whitney, Mineral magnetic and geochemical records of late Glacial climatic change from two northwest European carbonate lakes, *Journal of Paleolimnology* **22**(1999), pp. 97–107.

Nowaczyk, 2001 N.R. Nowaczyk, Logging of magnetic susceptibility. In: W.M. Last and J.P. Smol, Editors, *Tracking Environmental Change Using Lake Sediments* **Vol. 1**, Kluwer Academic Publisher, Dordrecht, The Netherlands (2001), pp. 155–170.

Olander, 1999 H. Olander, H.J.B. Birks, A. Korhola and T. Blom, An expanded calibration model for inferring lakewater and air temperatures from fossil chironomid assemblages in northern Fennoscandia, *The Holocene* **9** (1999), pp. 279–294.

Peyron et al., 1998 O. Peyron, J. Guiot, R. Cheddadi, P. Tarasov, M. Reille, J.L. de Beaulieu, S. Bottema and V. Andrieu, Climatic reconstruction in Europe for 18 000 yr BP from pollen data, *Quaternary Research* **49** (1998), pp. 183–196.

Peyron et al., 2000 O. Peyron, O. Jolly, R. Bonnefille, A. Vincens and J. Guiot, Climate of East Africa 6000 14C yr B.P., as inferred from pollen data, *Quaternary Research* **54** (2000), pp. 90–101.

Prentice et al., 1996 I.C. Prentice, J. Guiot, B. Huntley, D. Jolly and R. Cheddadi, Reconstructing biomes from palaeoecological data: a general method and its application to European pollen data at 0 and 6 ka, *Climate Dynamics* **12** (1996), pp. 185–194.

Quinlan and Smol, 2001 R. Quinlan and J.P. Smol, Chironomid-based inference models for estimating end-of-summer hypolimnetic oxygen from south-central Ontario shield lakes, *Freshwater Biology* **46** (2001), pp. 1529–1551.

Renssen and Bogaart, 2003 H. Renssen and P.W. Bogaart, Atmospheric variability over the 14.7 kyr BP stadial–interstadial transition in the North Atlantic region as simulated by an AGCM, *Climate Dynamics* **20** (2003), pp. 301–313.

Renssen and Isarin, 2001 H. Renssen and R.F.B. Isarin, The two major warming phases of the last deglaciation at 14,7 and 11,5 ka cal BP in Europe: climate reconstructions and AGCM experiments, *Global and Planetary Change* **30** (2001), pp. 117–153.

Saether, 1979 O.A. Saether, Chironomid communities as water quality indicators, *Holarctic Ecology* **2** (1979), pp. 65–74.

Sbaffi et al., 2004 L. Sbaffi, F.C. Wezel, G. Curzi and U. Zoppi, Millennial- to centennial-scale palaeoclimatic variations during Termination I and the Holocene in the central Mediterranean Sea, *Global and Planetary Change* **40** (2004), pp. 201–217.

Schmidt et al., 2002 R. Schmidt, C. van den Bogaard, J. Merkt and Müller, A new Lateglacial chronostratigraphic tephra marker for the south-eastern Alps: the Napolitan Yellow Tuff (NYT) in Längsee (Austria) in the context of a regional biostratigraphy and palaeoclimate, *Quaternary International* **88** (2002), pp. 45–56.

Schwander, 2000 J. Schwander, U. Eicher and B. Ammann, Stable isotopes of lake marl at Gerzensee and Leysin (Switzerland), covering the Younger Dryas and two minor oscillations, and their correlation to the GRIP ice core, *Palaeogeography, Palaeoecology, Palaeoclimatology* **159** (2000), pp. 215–230.

Sifeddine et al., 1998 A. Sifeddine, J. Bertaux, P. Mourguiart, L. Martin, J.R. Disnar and F. Laggoun-Defarge, Etude de la sédimentation lacustre d'un site de forêt d'altitude des Andes centrales (Bolivie). Implications paléoclimatiques, *Bulletin de la Société Géologique de France* **169** (1998), pp. 395–402.

Stockhausen and Zolitschka, 1999 H. Stockhausen and B. Zolitschka, Environmental changes since 13 000 cal. BP reflected in magnetic and sedimentological properties of sediments from Lake Holzmaar (Germany), *Quaternary Science Reviews* **18** (1999), pp. 913–925.

Stuiver et al., 1995 M. Stuiver, P.M. Grootes and T.F. Braziunas, The GISP2 $D^{18}O$ climate record of the past 16,500 years and the role of the sun, ocean and volcanoes, *Quaternary Research* **44** (1995), pp. 341–354.

Stuiver et al., 1998 M. Stuiver, P.J. Reimer, E. Bard, J.W. Beck, G.S. Burr, K.A. Hughen, B. Kromer, G. McCormac, J. van der Plicht and M. Spurk, Int cal 98 radiocarbon age calibration, 24 000–0 cal BP, *Radiocarbon* **40** (1998), pp. 1041–1083.

Ter Braak et al., 1998 Ter Braak, C.J.F., Smilauer, P., 1998. Canoco Reference Manual and User's Guide to Canoco of Windows. Centre for Biometry Wageningen.

Thompson and Oldfield, 1986 R. Thompson and F. Oldfield, Environmental Magnetism, Allen & Unwin, London (1986).

Thouveny et al., 1994 N. Thouveny, J.L. Beaulieu, E. Bonifay, K.M. Créer, J. Guiot, M. Icole, S. Johnsen, J. Jouzel, M. Reille, T. Williams and D. Williamson, Climate variations in Europe over the past 140 kyr deduced from rock magnetism, *Nature* **371** (1994), pp. 503–506.

Vandenberghe, 2003 J. Vandenberghe, Climate forcing of fluvial system development: an evolution of ideas, *Quaternary Science Reviews* **22** (2003), pp. 2053–2060.

Van Geel, 1996 B. Van Geel, Factors influencing changing AP/NAP ratios in NW-Europe during the Late-Glacial period, *Il Quaternario* **9** (1996), pp. 599–604.

Vanniere et al., 2004 B. Vanniere, G. Bossuet, A.V. Walter-Simonnet, P. Ruffaldi, T. Adatte, M. Rossy and M. Magny, High-resolution record of environmental changes and tephrochronological markers of the Last Glacial–Holocene transition at Lake Lautrey (Jura, France), *Journal of Quaternary Science* **19** (2004), pp. 797–808.

Vernet and Raynal, 2000 G. Vernet and J.P. Raynal, Un cadre tephrostratigraphique réactualisé pour la préhistoire tardiglaciaire et holocène de Limagne (Massif Central, France), *Comptes Rendus Académie des Sciences, Paris* **330** (2000), pp. 399–405.

Walker et al., 2003 M.J.C. Walker, G.R. Coope, C. Sheldrick, C.S.M. Turney, J.J. Lowe, S.P.E. Blockley and D.D. Harkness, Devensian Lateglacial environmental changes in Britain: a multi-proxy environmental record from Llanilid, South Wales, UK, *Quaternary Science Reviews* **22** (2003), pp. 475–520

Wiederholm, 1983 T. Wiederholm, Chironomidae of the Holarctic region. Keys and Diagnoses. Part 1. Larvae, *Entomologica Scandinavica Supplement* **19** (1983), pp. 1–457.

Wohlfarth et al., 1994 B. Wohlfarth, M.-J. Gaillard, W. Haeberli and K. Kelts, Environment and climate in southwestern Switzerland during the last termination, 15-10 ka BP, *Quaternary Science Reviews* **123** (1994), pp. 361–394.

Yu, 2000 Z. Yu, Ecosystem response to Lateglacial and early Holocene climate oscillations in the Great Lakes region of North America, *Quaternary Science Reviews* **19** (2000), pp. 1723–1747.